work was supported by a Grant-in-Aid from the Chinese Academy of Sciences (O514P51131 and KSCX1-YW-10), the Chinese 973 Project (2009CB522504), and the Chinese National Science and Technology Major Project (2008ZX10002-014).

## References


Aizaki, H., Lee, K.J., Sung, V.M., Ishiko, H., Lai, M.M., 2004. Characterization of the hepatitis C virus RNA replication complex associated with lipid rafts. Virology 324, 450–461.

Arnold, J.J., Cameron, C.E., 2000. Poliovirus RNA-dependent RNA polymerase (3D(pol)). Assembly of stable, elongation-competent complexes by using a symmetrical primer-template substrate (sym/sub). J. Biol. Chem. 275, 5329–5336.

Behrens, S.E., Tomei, L., De Francesco, R., 1996. Identification and properties of the RNA-dependent RNA polymerase of hepatitis C virus. EMBO J. 15, 12–22.

Binder, M., Quinkert, D., Bochkarova, O., Klein, R., Kezmic, N., Bartenschlager, R., Lohmann, V., 2007. Identification of determinants involved in initiation of hepatitis C virus RNA synthesis by using intergenotypic replicase chimeras. J. Virol. 81, 5270–5283.

Blight, K.J., McKeating, J.A., Marcotrigiano, J., Rice, C.M., 2003. Efficient replication of hepatitis C virus genotype 1a RNAs in cell culture. J. Virol. 77, 3181–3190.

Bressanelli, S., Tomei, L., Rey, F.A., De Francesco, R., 2002. Structural analysis of the hepatitis C virus RNA polymerase in complex with ribonucleotides. J. Virol. 76, 3482–3492.

Carroll, S.S., Sardana, V., Yang, Z., Jacobs, A.R., Mizenko, C., Hall, D., Hill, L., Zugay-Murphy, J., Kuo, L.C., 2000. Only a small fraction of purified hepatitis C RNA-dependent RNA polymerase is catalytically competent: implications for viral replication and in vitro assays. Biochemistry 39, 8243–8249.

Chinnaswamy, S., Murali, A., Li, P., Fujisaki, K., Kao, C.C., 2010. Regulation of de novo-initiated RNA synthesis in hepatitis C virus RNA-dependent RNA polymerase by intermolecular interactions. J. Virol. 84, 5923–5935.

Chinnaswamy, S., Yarbrough, I., Palaninathan, S., Kumar, C.T., Vijayaraghavan, V., Demeler, B., Lemon, S.M., Sacchettini, J.C., Kao, C.C., 2008. A locking mechanism regulates RNA synthesis and host protein interaction by the hepatitis C virus polymerase. J. Biol. Chem. 283, 20535–20546.

Clemente-Casares, P., Lopez-Jimenez, A.J., Bellon-Echeverria, I., Encinar, J.A., Martinez-Alfaro, E., Perez-Flores, R., Mas, A., 2011. De novo polymerase activity and oligomerization of hepatitis C virus RNA-dependent RNA-polymerases from genotypes 1 to 5. *PLoS One* 6, *e18515*.

Cramer, J., Jaeger, J., Restle, T., 2006. Biochemical and pre-steady-state kinetic characterization of the hepatitis C virus RNA polymerase (NS5BDelta21, HC-J4). Biochemistry 45, 3610–3619.

Fernandez-Recio, J., Vazquez, A., Civera, C., Sevilla, P., Sancho, J., 1997. The tryptophan/histidine interaction in alpha-helices. J. Mol. Biol. 267, 184–197.

Ferrari, E., Wright-Minogue, J., Fang, J.W., Baroudy, B.M., Lau, J.Y., Hong, Z., 1999. Characterization of soluble hepatitis C virus RNA-dependent RNA polymerase expressed in *Escherichia coli*. J. Virol. 73, 1649–1654.

Grakoui, A., McCourt, D.W., Wychowski, C., Feinstone, S.M., Rice, C.M., 1993. Characterization of the hepatitis C virus-encoded serine proteinase: determination of proteinase-dependent polyprotein cleavage sites. J. Virol. 67, 2832–2843.

Hijikata, M., Mizushima, H., Tanji, Y., Komoda, Y., Hirowatari, Y., Akagi, T., Kato, N., Kimura, K., Shimotohno, K., 1993. Proteolytic processing and membrane association of putative nonstructural proteins of hepatitis C virus. Proc. Natl. Acad. Sci. U. S. A. 90, 10773–10777.

Hirschman, S.Z., Gerber, M., Garfinkel, E., 1978. Differential activation of hepatitis B DNA polymerase by detergent and salt. J. Med. Virol. 2, 61–76.

Hong, Z., Cameron, C.E., Walker, M.P., Castro, C., Yao, N., Lau, J.Y., Zhong, W., 2001. A novel mechanism to ensure terminal initiation by hepatitis C virus NS5B polymerase. Virology 285, 6–11.

Kashiwagi, T., Hara, K., Kohara, M., Iwahashi, J., Hamada, N., Honda-Yoshino, H., Toyoda, T., 2002a. *Promoter/origin structure of the complementary strand of hepatitis C* virus genome. J. Biol. Chem. 277, 28700–28705.

Kashiwagi, T., Hara, K., Kohara, M., Kohara, K., Iwahashi, J., Hamada, N., Yoshino, H., Toyoda, T., 2002b. Kinetic analysis of C-terminally truncated RNA-dependent RNA polymerase of hepatitis C virus. Biochem. Biophys. Res. Commun. 290, 1188–1194.

Kiyosawa, K., Sodeyama, T., Tanaka, E., Gibo, Y., Yoshizawa, K., Nakano, Y., Furuta, S., Akahane, Y., Nishioka, K., Purcell, R.H., et al., 1990. Interrelationship of blood transfusion, non-A, non-B hepatitis and hepatocellular carcinoma: analysis by detection of antibody to hepatitis C virus. Hepatology 12, 671–675.

Lemon, S., Walker, C., Alter, M., Yi, M., 2007. Hepatitis C virus. In: Knipe, D., Howley, P. (Eds.), *Fields Virology*. Lippincott-Raven Publishers, Philadelphia, PA, pp. 1253–1304.

Lohmann, V., Korner, F., Herian, U., Bartenschlager, R., 1997. Biochemical properties of hepatitis C virus NS5B RNA-dependent RNA polymerase and identification of amino acid sequence motifs essential for enzymatic activity. J. Virol. 71, 8416–8428.

Luo, G., Hamatake, R.K., Mathis, D.M., Racela, J., Rigat, K.L., Lemm, J., Colonno, R.J. De, 2000. novo initiation of RNA synthesis by the RNA-dependent RNA polymerase (NS5B) of hepatitis C virus. J. Virol. 74, 851–863.

Marti, D.N., Bosshard, H.R., 2003. Electrostatic interactions in leucine zippers: thermodynamic analysis of the contributions of Glu and His residues and the effect of mutating salt bridges. J. Mol. Biol. 330, 621–637.

Matthews, J.M., Ward, L.D., Hammacher, A., Norton, R.S., Simpson, R.J., 1997. Roles of histidine 31 and tryptophan 34 in the structure, self-association, and folding of murine interleukin-6. Biochemistry 36, 6187–6196.

Murayama, A., Date, T., Morikawa, K., Akazawa, D., Miyamoto, M., Kaga, M., Ishii, K., Suzuki, T., Kato, T., Mizokami, M., Wakita, T., 2007. The NS3 helicase and NS5B-to-3′X regions are important for efficient hepatitis C virus strain JFH-1 replication in Huh7 cells. J. Virol. 81, 8030–8040.

Murayama, A., Weng, L., Date, T., Akazawa, D., Tian, X., Suzuki, T., Kato, T., Tanaka, Y., Mizokami, M., Wakita, T., Toyoda, T., 2010. RNA polymerase activity and specific RNA structure are required for efficient HCV replication in cultured cells. PLoS Pathog. 6, e1000885.

Qin, W., Luo, H., Nomura, T., Hayashi, N., Yamashita, T., Murakami, S., 2002. Oligomeric *interaction of hepatitis C virus NS5B is critical for catalytic activity of RNA*-dependent RNA polymerase. J. Biol. Chem. 277, 2132–2137.

Ranjith-Kumar, C.T., Gajewski, J., Gutshall, L., Maley, D., Sarisky, R.T., Kao, C.C., 2001. Terminal nucleotidyl transferase activity of recombinant Flaviviridae RNA-dependent RNA polymerases: implication for viral RNA synthesis. J. Virol. 75, 8615–8623.

Ranjith-Kumar, C.T., Sarisky, R.T., Gutshall, L., Thomson, M., Kao, C.C. De, 2004. novo initiation pocket mutations have multiple effects on hepatitis C virus RNA-dependent RNA polymerase activities. J. Virol. 78, 12207–12217.

Saito, I., Miyamura, T., Ohbayashi, A., Harada, H., Katayama, T., Kikuchi, S., Watanabe, Y., Koi, S., Onji, M., Ohta, Y., et al., 1990. Hepatitis C virus infection is associated with the development of hepatocellular carcinoma. Proc. Natl. Acad. Sci. U. S. A. 87, 6547–6549.

Sakamoto, H., Okamoto, K., Aoki, M., Kato, H., Katsume, A., Ohta, A., Tsukuda, T., Shimma, N., Aoki, Y., Arisawa, M., Kohara, M., Sudoh, M., 2005. Host sphingolipid biosynthesis as a target for hepatitis C virus therapy. Nat. Chem. Biol. 1, 333–337.

Schmitt, M., Scrima, N., Radujkovic, D., Caillet-Saguy, C., Simister, P.C., Friebe, P., Wicht, O., Klein, R., Bartenschlager, R., Lohmann, V., Bressanelli, S., 2011. A comprehensive structure–function comparison of hepatitis C virus strain JFH1 and J6 polymerases reveals a key residue stimulating replication in cell culture across genotypes. J. Virol. 85, 2565–2581.

Shi, S.T., Lee, K.J., Aizaki, H., Hwang, S.B., Lai, M.M., 2003. Hepatitis C virus RNA replication occurs on a detergent-resistant membrane that cofractionates with caveolin-2. J. Virol. 77, 4160–4168.

Simister, P., Schmitt, M., Geitmann, M., Wicht, O., Danielson, U.H., Klein, R., Bressanelli, S., Lohmann, V., 2009. Structural and functional analysis of hepatitis C virus strain JFH1 polymerase. J. Virol. 83, 11926–11939.

Takeuchi, H., Okada, A., Miura, T., 2003. Roles of the histidine and tryptophan side chains in the M2 proton channel from influenza A virus. FEBS Lett. 552, 35–38.

Tanaka, T., Kato, N., Cho, M.J., Sugiyama, K., Shimotohno, K., 1996. Structure of the 3′ terminus of the hepatitis C virus genome. J. Virol. 70, 3307–3312.

Thompson, F.M., Libertini, L.J., Joss, U.R., Calvin, M., 1972. Detergent effects on a reverse transcriptase activity and on inhibition by rifamycin derivatives. Science 178, 505–507.

Tsukiyama-Kohara, K., Iizuka, N., Kohara, M., Nomoto, A., 1992. Internal ribosome entry site within hepatitis C virus RNA. J. Virol. 66, 1476–1483.

Vo, N.V., Tuler, J.R., Lai, M.M., 2004. Enzymatic characterization of the full-length and C-terminally truncated hepatitis C virus RNA polymerases: function of the last 21 amino acids of the C terminus in template binding and RNA synthesis. Biochemistry 43, 10579–10591.

Wang, Q.M., Hockman, M.A., Staschke, K., Johnson, R.B., Case, K.A., Lu, J., Parsons, S., Zhang, F., Rathnachalam, R., Kirkegaard, K., Colacino, J.M., 2002. Oligomerization and cooperative RNA synthesis activity of hepatitis C virus RNA-dependent RNA polymerase. J. Virol. 76, 3865–3872.

Wasley, A., Alter, M.J., 2000. Epidemiology of hepatitis C: geographic differences and temporal trends. Semin. Liver Dis. 20, 1–16.

Watashi, K., Ishii, N., Hijikata, M., Inoue, D., Murata, T., Miyanari, Y., Shimotohno, K., 2005. Cyclophilin B is a functional regulator of hepatitis C virus RNA polymerase. Mol. Cell 19, 111–122.

Weng, L., Du, J., Zhou, J., Ding, J., Wakita, T., Kohara, M., Toyoda, T., 2009. Modification of hepatitis C virus 1b RNA polymerase to make a highly active JFH1-type polymerase by mutation of the thumb domain. Arch. Virol. 154, 765–773.

Weng, L., Hirata, Y., Arai, M., Kohara, M., Wakita, T., Watashi, K., Shimotohno, K., He, Y., Zhong, J., Toyoda, T., 2010. Sphingomyelin activates hepatitis C virus RNA polymerase in a genotype specific manner. J. Virol. 84, 11761–11770.

Weyant, R.S., Edmonds, P., Swaminathan, B., 1990. Effect of ionic and nonionic detergents on the Taq polymerase. Biotechniques 9, 308–309.

Wu, A.M., Cetta, A., 1975. On the stimulation of viral DNA polymerase activity by nonionic detergent. Biochemistry 14, 789–795.

SCIENTIFIC REPORTS

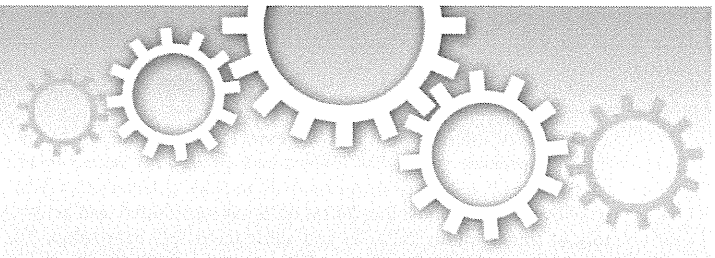

OPEN

SUBJECT AREAS:
GENE REGULATION
VIROLOGY
PATHOGENS
RNAI

Received
7 November 2011

Accepted
23 January 2012

Published
10 February 2012

Correspondence and requests for materials should be addressed to M.S. (sudomsy@chugai-pharm.co.jp)

# An orally available, small-molecule interferon inhibits viral replication

Hideyuki Konishi[1], Koichi Okamoto[1], Yusuke Ohmori[1], Hitoshi Yoshino[2], Hiroshi Ohmori[1], Motooki Ashihara[1], Yuichi Hirata[3], Atsunori Ohta[1], Hiroshi Sakamoto[1], Natsuko Hada[1], Asao Katsume[1], Michinori Kohara[3], Kazumi Morikawa[2], Takuo Tsukuda[1], Nobuo Shimma[1], Graham R. Foster[4], William Alazawi[4], Yuko Aoki[1], Mikio Arisawa[1] & Masayuki Sudoh[1]

[1]Kamakura Research Laboratories, Chugai Pharmaceutical Co. Ltd., Kamakura, Kanagawa, Japan, [2]Fuji-Gotemba Research Laboratories, Chugai Pharmaceutical Co. Ltd., Gotemba, Shizuoka, Japan, [3]Department of Microbiology and Cell Biology, The Tokyo Metropolitan Institute of Medical Science, Setagaya-ku, Tokyo, Japan, [4]Queen Mary University of London, Blizard Institute of Cellular and Molecular Science, 4 Newark Street, London E1 4AT, UK.

**Most acute hepatitis C virus (HCV) infections become chronic and some progress to liver cirrhosis or hepatocellular carcinoma. Standard therapy involves an interferon (IFN)-α-based regimen, and efficacy of therapy has been significantly improved by the development of protease inhibitors. However, several issues remain concerning the injectable form and the side effects of IFN. Here, we report an orally available, small-molecule type I IFN receptor agonist that directly transduces the IFN signal cascade and stimulates antiviral gene expression. Like type I IFN, the small-molecule compound induces IFN-stimulated gene (ISG) expression for antiviral activity *in vitro* and *in vivo* in mice, and the ISG induction mechanism is attributed to a direct interaction between the compound and IFN-α receptor 2, a key molecule of IFN-signaling on the cell surface. Our study highlights the importance of an orally active IFN-like agent, both as a therapy for antiviral infections and as a potential IFN substitute.**

Hepatitis C virus (HCV) infection affects 170 million people worldwide[1], and most acute HCV infections become chronic, with some progression to liver cirrhosis or hepatocellular carcinoma. HCV has a plus-strand RNA genome that encodes both structural proteins and the nonstructural (NS) proteins 2, 3, 4A, 4B, 5A and 5B. Current standard therapy against chronic HCV infection includes the use of host factor-targeting pegylated interferon (PEG-IFN)-α and ribavirin[2], which is effective in only 50% of patients chronically infected with HCV genotype 1[3]. The main causes of this low rate of efficacy may be (i) single-nucleotide polymorphisms (SNPs) in the upstream region of the *IL28B* gene and (ii) low compliance with the therapy, which must be administered subcutaneously. Regarding the first cause—SNPs—the host factors that are important in the early response to therapy remain unknown. However, recent studies report that genetic variants near *IL28B*, which encodes IFN-λ3 (interleukin 28B), correlate with the response to treatment of chronic hepatitis C infection using IFN-α/ribavirin combination therapy[4–7]. Patients with an rs12979860 SNP genotype of CC are reported to have a stronger response to IFN therapy (up to an 80% sustained virological response (SVR) rate with the combined therapy) than those with TC or TT genotypes[4]. Regarding the lack of compliance, the current therapy using recombinant IFN is a weekly injectable formulation that is unstable, requires refrigeration, and is expensive and complex to administer. Furthermore, therapy is often poorly tolerated as a result of the presence of many adverse effects, including flu-like symptoms, hematological abnormalities and adverse neuropsychiatric events, any of which may require early discontinuation[8]. These side effects may result in dose modifications that lead to less-than-optimal responses.

Recent trends in drug development focus on drugs targeted against viral proteins such as NS 3/4A serine protease, RNA helicase, NS4B, NS5A, and NS5B RNA-dependent RNA polymerase[9]. Very recently, two NS3/4A protease inhibitors, telaprevir and boceprevir, have been approved as new anti-HCV agents. Adding such an inhibitor to the standard therapy in the ADVANCE[10] and the SPRINT-2[11] trials achieved significantly higher SVR rates, but the issue still remains that using these inhibitors without injectable IFN possibly yields clinical resistance[12]. To overcome this problem and alleviate the low compliance outlined above, an orally available IFN would be valuable because the dosing regimen is less complex.

IFNs induce the expression of a subset of IFN-stimulated genes (ISG)[13], some of which show antiviral activity or are involved in lipid metabolism, apoptosis, protein degradation and inflammation[14]. IFNs are not only effective

against HCV infection, but are also essential for innate immunity. Broadly speaking, type I IFNs (IFN-α and -β) bind to their receptor, causing the phosphorylation and activation of JAK1 and Tyk2, which is followed by the phosphorylation of signal transducers and activators of transcription (STATs) and subsequent ISG expression. To activate the JAK/STAT pathway, IFN-α requires the IFN-α/β receptor, which consists of 2 subunits, IFN-α receptor (IFNAR) 1 and IFNAR2. These IFNAR subunits together form a heterodimer upon IFN stimulation. This association of IFNAR2 and IFNAR1 is required to mediate the antiviral, antiproliferative, and apoptotic effects of type I IFNs[15–17] because the dimerization of IFNARs induces the phosphorylation of the receptor-associated tyrosine kinases, JAK1 and Tyk2, and the phosphorylated JAK kinases then phosphorylate STAT1 and STAT2. In turn, phosphorylated STAT1 and STAT2 bind to IRF9 to form the transcriptional activator IFN-stimulating gene factor 3 (ISGF3) that induces the expression of a subset of ISGs[13].

Using quantitative high-throughput screening (HTS), we identified in this study a novel small molecule that acts like IFN by directly interacting with the type I IFN receptor to drive ISG expression. Our results indicate that oral administration of the small-molecule IFN agonist stimulates ISG expression in mice, and that the ISG expression from this small-molecule IFN provides antiviral activity, indicating that the compound may be a potential therapeutic IFN substitute.

## Results

**Identification of antiviral small-molecule IFN agonists by high-throughput chemical library screening.** HCV replicon cells, which were established ten years ago[18] using a cell line that expresses the HCV genotype 1b subgenomic replicon[19], possess a luciferase gene as a reporter optimized for use in a robust HTS system. The HTS system provides in-depth analysis of primary screening results, including detailed information regarding potency, efficacy and structure-activity relationships. IFNs show strong inhibition using this system and have been used as a positive control in the assay. Many compounds, including HCV protease inhibitors and HCV polymerase nucleoside/non-nucleoside analogs, have been assessed and are being developed for clinical testing. Analysis of data from the combination of target/counterscreen HTS, data from other assays measuring cellular toxicity, *in vitro* sphingolipid biosynthesis and HCV enzymatic activity (including protease and polymerase) allowed us to select compounds with potentially novel modes of action from the primary screen.

A secondary IFN signal assay, using a luciferase reporter gene which was located downstream of the IFN-stimulated response element (ISRE), eliminated assay-related false-positive compounds. Of the remaining anti-HCV replicon compounds, one of the most active was an imidazonaphthyridine with the structural formula 8-(1, 3, 4-oxadiazol-2-yl)-2, 4-bis (trifluoromethyl) imidazo [1, 2-a] [1, 8] naphthyridine (RO4948191, hereinafter RO8191) (Fig. 1a). This compound strongly suppressed HCV replicon activity at 72 h in a dose-dependent manner (Fig. 1b, left graph) without inducing host cell toxicity, as measured by the WST-8 (Fig. 1b, right graph) and CellTiter-Glo assays (data not shown). The $IC_{50}$ (50% inhibitory concentration) of the compound in an anti-HCV replicon assay was 200 nM. The compound suppressed viral replication within 24 h and showed even more effective inhibition, without cytotoxicity, after 7 days (Supplementary Fig. 1). In addition, the HCV RNA replicon levels significantly decreased after incubation with the compound for 72 h, as determined by real-time reverse transcription (RT)-polymerase chain reaction (PCR) analysis (Fig. 1c). Immunostaining showed that levels of the proteins HCV NS3 and NS4A, which are localized mainly in the perinuclear region of the replicon cells, were also reduced after RO8191 treatment for 24 h (Fig. 1d). This treatment also resulted in the disappearance of viral proteins such as NS3, NS4A/B, and NS5A/B, as shown by western blot analysis (Fig. 1e). The luciferase activity of HCV subgenomic genotype 2 replicon cells (JFH1, data not shown) and, surprisingly, the HCV viral titer of JFH1[20] in a Huh-7/K4 cell line were also reduced by RO8191 treatment (Fig. 1f).

**RO8191 induces IFN signals, ISGs expression and JAK/STAT phosphorylation.** To clarify whether RO8191 shows inhibitory activity against another RNA virus, we tested its action in encephalomyocarditis virus (EMCV)-infected A549 cells. RO8191 showed a cell-protective activity against EMCV infection similar to that of IFN-α (Fig. 2a). Because IFN-α is the most common host cell factor to exert its antiviral activity against HCV[21,22] by inducing ISG expression[13], we compared the gene expression profiles of IFN-α and RO8191 by conducting a global-scale DNA microarray analysis to identify genes, especially ISGs[23], that were regulated by RO8191. As expected, RO8191 increased the expression of some ISGs (Supplementary Fig. 2 and Supplementary Table 1). DNA microarray analysis showed that RO8191 induced the expression of IP-10 (CXCL10), known as an ISG, RO8191 did not induce the genes encoding inflammatory cytokines and chemokines (Supplementary Fig. 3a). And, a reporter gene assay was performed using an NF-κB reporter gene. We transiently transfected the reporter gene to HCV-naïve HuH-7 cells, and then treated them with RO8191 or TNF-α. In Huh-7 cells, NF-κB reporter gene was activated by TNF-α treatment, but not by RO8191 (Supplementary Fig. 3b). These results indicate that RO8191 specifically induces the IFN-relevant gene expressions.

Real-time RT-PCR analysis also revealed that RO8191 induced many ISGs similar to those expressed in IFN-α-treated cells (Fig. 2b and Supplementary Table 2), suggesting that the antiviral mechanism of RO8191 depends on ISG expression. In addition to HCV replicon cells, we tested the compound in several cancer cell lines and normal human primary hepatocytes (Hc cells). Real-time RT-PCR analysis showed that RO8191 induced ISG expression in cultured cell lines and human primary hepatocytes (Supplementary Table 3 and Supplementary Fig. 4). These results suggest that RO8191 induces an IFN signal, and that the application in clinical of RO8191 is not limited to suppressing HCV infection.

As mentioned earlier, type I IFNs phosphorylate JAK kinases and STAT proteins by inducing a heterodimerization of both IFNAR1 and IFNAR2, and the complexes thus formed transduce signals from IFN. Since RO8191 induces ISGs in a similar profile to IFN-α, we examined the phosphorylation of IFN signaling molecules. Immunoblotting analysis was performed to detect phosphorylated tyrosine (Tyr) and serine (Ser) residues of the STATs and JAK kinases using cell lysate that was treated with 50~5000 times the HCV replicon $IC_{50}$s of RO8191, IFN-α, IFN-β, and IFN-γ (type II IFN). The degree to which both RO8191 and IFN-β phosphorylated STAT1, STAT5, and STAT6 was similar, as shown in Fig. 2c, and the phosphorylation level of STAT2 by RO8191 was quite similar to that of IFN-α. Interestingly, STAT3 and JAK1 were more strongly phosphorylated by RO8191 than by IFN-α, -β, or -γ. On the other hand, Tyk2 was phosphorylated by type I IFNs, but not by IFN-γ or RO8191, indicating that Tyk2 is dispensable for RO8191 activity (Fig. 2c). Taken together, the phosphorylation profile of STAT proteins by RO8191 is generally similar to that of type I IFNs, and the phosphorylation profiles of STAT1–3, 5, 6, and JAK1 in HCV replicon cells treated with RO8191 or type I IFNs suggest a common mechanism that differs from the mechanism in cells treated with type II IFN.

In addition to imiquimod, an IFN inducer and a Toll-like receptor (TLR) 7 agonist[24], small-molecule ligands recognized by TLRs and RIG-I–like receptors are known to induce ISG expression by inducing IFN[25]. The chemical structure of RO8191 is similar to imiquimod so we examined whether RO8191 has a mechanism of activity like imiquimod. However, imiquimod did not affect HCV replicon cells (Supplementary Fig. 5a) and, moreover, did not stimulate

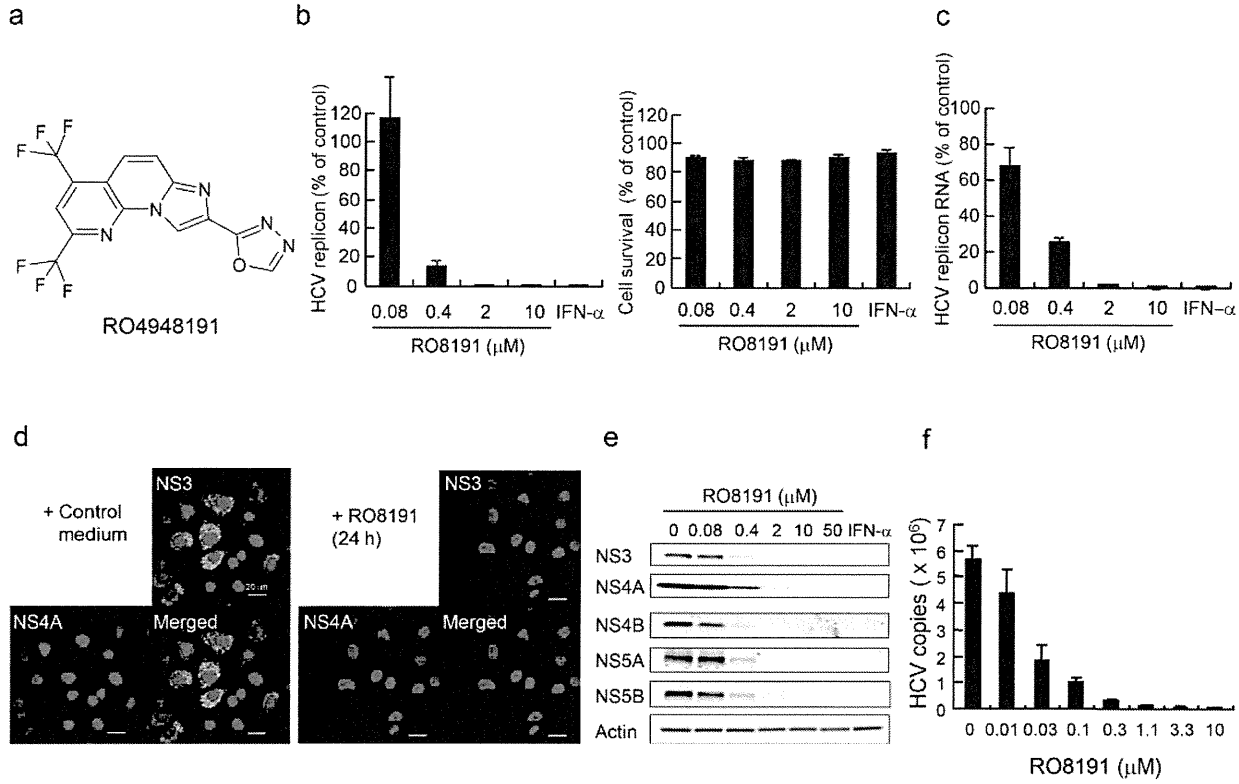


**Figure 1 | Identification of a small molecule that inhibits HCV replication.** (a) The chemical structure of RO8191. (b) After treatment with various concentrations of RO8191 or 100 IU/mL IFN-α for 72 h, HCV replication levels were examined using a luciferase assay (left graph), and cell viabilities were determined using a WST-8 assay (right graph). The mean values and their SDs were recorded for treated cells as a percentage of the values for untreated cells, and the values represent the means of 3 independent experiments. (c) Total RNA was extracted from HCV replicon cells cultured with the indicated concentration of RO8191 or 100 IU/mL IFN-α for 72 h; HCV RNA levels were analyzed using real-time RT-PCR. The mean values and their SDs were recorded for treated cells relative to the mRNA levels of β-actin, and are shown as a percentage of untreated cells. The values represent the means of 3 independent experiments. (d) HCV replicon cells were treated with control medium (left panels) or 10 μM RO8191 (right panels) for 24 h and immunostained with Hoechst 33452 (blue), anti-NS3 antibody (green), and anti-NS4A antibody (red). The results were then merged (yellow). (e) HCV replicon cells were treated with the indicated concentrations of RO8191 or 100 IU/mL IFN-α for 72 h. Whole cell lysates were immunoblotted with antibodies specific to the indicated HCV NS proteins. (f) After infection with the HCV JFH1 strain, Huh-7/K4 cells were treated with the indicated concentrations of RO8191 for 72 h. Total RNA was extracted, and the HCV RNA levels were analyzed using quantitative real-time RT-PCR.

STAT1 phosphorylation, whereas RO8191 caused prolonged STAT1 activation (for up to 8 h post-treatment; Supplementary Fig. 5b). Next, RO8191 is actually a small-molecule and we could not exclude the possibility that the antiviral activity might be induced through TLRs. To confirm that, we tested ISG induction using Tlr3, 4, 7 and 9 knockout (KO) mouse embryo fibroblasts (MEF)[24,26–28]. We treated the MEFs with RO8191 or murine IFN-αA for 8 h and both induced Oas1b mRNA in wild type and Tlr-KO MEFs (Supplementary Fig. 5c), demonstrating that RO8191 induces ISG expressions independently of TLRs. To exclude the possibility that RO8191 acts by inducing type I IFN, we examined its effects in Vero cells that lack the IFN gene locus[29,30]. Whereas imiquimod did not show IFN-like effects in Vero cells, RO8191 and IFN-α induced the ISRE activation (Supplementary Fig. 5d), indicating that RO8191 acts independently of the inducing IFN and is quite distinct from imiquimod.

**RO8191 exerts antiviral activity dependent on IFNAR2/JAK1, but is independent of IFNAR1/Tyk2.** IFNs require IFN receptor subunits for their activity, and we hypothesized that RO8191 uses the IFN receptor to exert anti-HCV activity. To determine the contributions of IFNAR1 and IFNAR2 toward the anti-HCV replicon activity of RO8191, we suppressed the expression of these receptors using specific siRNA and treated the cells with RO8191 or IFN-α. The knockdown efficiency was determined using RT-PCR in the HCV replicon cells transfected with each siRNA, as shown in Supplementary Fig. 6. As expected, a knockdown of each receptor subunit decreased the antiviral activity of IFN-α (Fig. 3a and b, Supplementary Fig. 7a and b). IFNAR2 knockdown attenuated the antiviral activity of RO8191 (Fig. 3b and Supplementary Fig. 7b) but, interestingly, IFNAR1 knockdown did not change the antiviral activity (Fig. 3a and Supplementary Fig. 7a), suggesting that RO8191 is independent of IFNAR1. To address whether IFN-α receptor contributes to RO8191 signaling, we evaluated RO8191 using Ifnar1-KO MEF cells[31]. We treated Ifnar1-KO MEFs with 50 μM RO8191 or 1,000 IU/mL of murine IFN-αA for 8 h and analyzed the expression of murine *Oas1b* mRNA using real-time RT-PCR. Murine IFN induced murine *Oas1b* mRNA only in wild type MEFs, not in Ifnar1-KO MEFs, although RO8191 induced *Oas1b* in both wild type and Ifnar1-KO MEFs (Supplementary Fig. 8). Therefore, RO8191 induces IFN-like activity even in Ifnar1-KO MEFs.

Since IFNAR2 knockdown reduced RO8191 activity, we focused on and analyzed the IFNAR2 function using RO8191. First, U5A cells, which do not respond to IFN-α because of the lack of

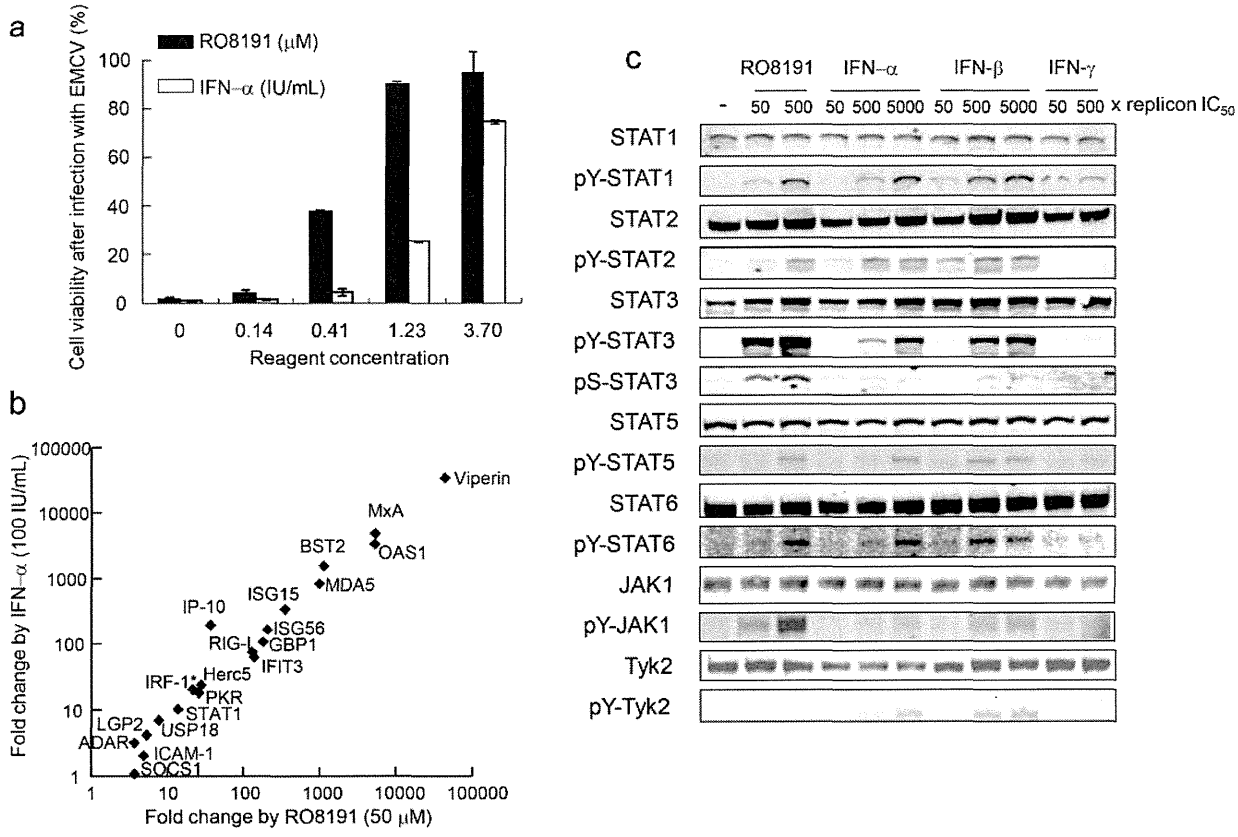


**Figure 2 | RO8191 activates JAK/STAT and induces IFN-like signals.** (a) The cytopathic effect of EMCV infection was inhibited by the indicated concentrations of RO8191 or IFN-α. Viable cells were stained with crystal violet. The data shown are the mean values and SDs based on experiments performed in quadruplicate. (b) ISG expression levels were measured using real-time RT-PCR. Total RNA was extracted from HCV replicon cells cultured in the presence of 50 μM RO8191 or 100 IU/mL IFN-α for 2 or 8 h and known ISGs were analyzed. Asterisk indicates 2-h treatment with agents. The values shown are the mean fold change induction compared to the mRNA level of human *β-actin* and the fold change induction compared to untreated cells. (c) HCV replicon cells were treated with various concentrations of the indicated agents for 15 min. Total lysates were immunoblotted with antibodies to STATs or JAK kinases. The HCV replicon $IC_{50}$ of IFN-α was 0.4 IU/mL, that of IFN-β was 3 IU/mL, and that of IFN-γ was 0.3 ng/mL.

IFNAR2 expression[32], were treated with RO8191. Although RO8191 and IFN-α did not induce *OAS1* expression in the U5A cells, IFNAR2-overexpressing U5A cells were successfully complemented, and this conferred susceptibility to both RO8191 and IFN-α (Fig. 3c and d). RO8191 also induced the *OAS1* gene in HT1080 and 2fTGH cells, the parental cell lines of U5A cells (Supplementary Table 3, lowest and second lowest rows). Second, to elucidate whether RO8191 directly interacts with IFNAR2, we obtained a recombinant IFNAR2 extracellular domain (ECD) protein (N-terminal half of the protein, amino acids from Ile27- Lys243). The protein was subjected to surface plasmon resonance (SPR) spectroscopy using a Biacore system to directly evaluate the binding activity of the recombinant protein with its possible ligands, RO8191 and IFN-α. The IFNAR2 ECD protein was fixed on the surface of the CM7 sensor chip by amine coupling, and PEG-IFN-α2a and RO8191 were injected as analytes. We comparatively analyzed 0.31 and 0.63 μM of RO8191, and both concentrations showed similar binding affinities of 480.5 and 484.5 nM, respectively (Fig. 3e), whereas a chemically derivatized compound of RO8191 that cannot inhibit HCV replication did not bind to IFNAR2 ECD (data not shown). The SPR results were consistent with 1:1 binding and showed an interaction between RO8191 and the IFNAR2 ECD protein in a dose-dependent manner, indicating that the compound and IFNAR2 may directly interact on the cell surface. In addition to the anti-replicon activity, the phosphorylation of STAT1 by RO8191 was also repressed by IFNAR2 knockdown (Fig. 3g), but the knockdown of IFNAR1 did not inhibit the STAT1 phosphorylation (Fig. 3f), indicating that RO8191 requires IFNAR2 but not IFNAR1 to achieve activity. Similarly, the knockdown of JAK1 attenuated the activity of RO8191 and IFN-α (Fig. 4a and Supplementary Fig. 9a), while, in contrast, Tyk2 and JAK2 were not required for RO8191 activity (Fig. 4b, Supplementary Fig. 9b and c). The phosphorylation of STAT1 by RO8191 was also inhibited by a knockdown of JAK1 (Supplementary Fig. 10a), but not by a knockdown of Tyk2 (Supplementary Fig. 10b), indicating JAK1 essentiality for the antiviral activity of RO8191. To confirm Tyk2-independency, we used U1A (Tyk2-deficient) cells and the parental cell, 2fTGH[33], and treated them with 50 μM RO8191 or 100 IU/mL IFN-α for 8 h to analyze the expression of *OAS1*. As expected from previous reports[34], IFN-α induced the *OAS1* expression only in 2fTGH cells but not in U1A cells; however, RO8191 induced the expression in both 2fTGH and U1A cells significantly (Supplementary Fig. 11). Thus, RO8191 activates ISGs in a JAK1-dependent and Tyk2-independent manner; on the other hand, IFN-α depends on both factors. Next, we conducted a knockdown of the transcription factors related to type I IFNs activity, STAT1, STAT2 and IRF-9, to clarify whether RO8191 required these factors for antiviral activity. As expected, STAT1-siRNAs partially blocked IFN-γ activity (Supplementary Fig. 9d),

Table 1 | ISG expression in the livers of RO8191 treated mice. ISG expression levels were measured using real-time RT-PCR. Values are listed relative to the mRNA levels of rodent *Gapdh* and represent the mean fold change induction compared to vehicle-administered mice. Twenty-four hours after oral administration of 30 mg/kg RO8191 or vehicle (including 10% dimethyl sulfoxide and 10% Cremophor) to mice, total RNA was extracted from the mouse livers, and the mRNA levels of murine ISGs were measured using real-time RT-PCR. The data shown are the means and SDs of 4 mice per group. The data were statistically analyzed using Student's *t*-test, and differences were considered significant at p values $< 0.05$

| Gene | Entrez ID | Fold change ± SD | | | p-value |
|---|---|---|---|---|---|
| murine Oas1 | NM_001083925 | 3.0 | ± | 0.72 | 0.003 |
| murine Mx1 | NM_010846 | 2.1 | ± | 0.15 | 0.0003 |
| murine Pkr | NM_011163 | 1.4 | ± | 0.21 | 0.009 |
| murine Cxcl10 | NM_021274 | 1.7 | ± | 0.63 | 0.097 |
| murine Ifit3 | NM_010501 | 2.5 | ± | 0.48 | 0.001 |
| murine Isg15 | NM_015783 | 2.3 | ± | 0.41 | 0.002 |
| murine Mda5 | NM_027835 | 1.6 | ± | 0.22 | 0.003 |
| murine Rig-i | NM_172689 | 2.1 | ± | 0.16 | 0.00003 |
| murine Socs1 | NM_009896 | 2.6 | ± | 1.04 | 0.057 |
| murine Stat1 | NM_009283 | 1.8 | ± | 0.21 | 0.001 |
| murine Usp18 | NM_011909 | 2.6 | ± | 0.69 | 0.017 |

which is mediated by STAT1 homodimers[35]. STAT1 was significantly phosphorylated by both RO8191 and IFN-α (Fig. 2c); however, the STAT1 knockdown affected neither RO8191 nor IFN-α activity (Fig. 4c and Supplementary Fig. 9d). We also analyzed the impact of STAT1 knockdown on *OAS1* induction by RO8191, and found *OAS1* induction by RO8191 was inhibited (Supplementary Fig. 12). STAT2 and IRF9 knockdown attenuated the inhibitory activity of both RO8191 and IFN-α (Fig. 4d and e and Supplementary Fig. 9e and f). In summary, RO8191 only binds to IFNAR2 and activates JAK1, STATs, and IRF9, thereby exhibiting type I IFN-like activity (Fig. 4f).

**RO8191, an IFNAR2 agonist, stimulates IFN signals in mice.** To evaluate whether RO8191 could be a clinical lead for drug development, we studied the effects of RO8191 on IFN signaling in mice. The compound or vehicle was orally administered to mice and, 24 h after treatment, the liver was removed and examined. The antiviral genes *Oas1b*, *Mx1*, and *Pkr* were significantly induced in the livers of mice treated with RO8191 (Table 1). As expected, gene homologs that were induced in the livers of HCV patients treated with PEG-IFN-α2b[36] were also induced in mouse liver (*Ifit3*, *Isg15*, *Mda5*, *Rig-I*, *Socs1* and *Stat1*; Table 1). In addition, genes that had previously been reported to be induced by IFN-β in mouse liver[37] were also induced in the livers of RO8191-treated mice (*Cxcl10*, *Ifit3*, *Isg15*, *Socs1* and *Usp18*; Table 1,). We also measured inflammatory cytokine and chemokine expressions, and RO8191 did not significantly induce the expression of these genes (Supplementary Table 4). To evaluate anti-HCV activity of RO8191 *in vivo*, RO8191 was orally administered to HCV-infected humanized liver mice[38]. The results of this humanized liver mice study showed that RO8191 reduced HCV titer *in vivo* (Supplementary Fig. 13). These data show that RO8191 stimulates IFN signaling and is an orally available agent in mice.

## Discussion

In this study, we identified a small-molecule IFN receptor agonist, RO8191, by quantitative HTS of a chemical library. This compound showed antiviral activity against both HCV and EMCV, suggesting a broad spectrum of target viruses. To learn more about the possible mechanism of action of IFN signal induction by RO8191, we investigated IFN-induced signaling and ISG induction by the small-molecule compound *in vitro* and *in vivo*. A comparison of microarray expression profiles in HCV replicon cells stimulated by IFN-α or RO8191 indicates that the IFN signal was induced not only by IFNs, but also by the small-molecule compound (Fig. 2b and Supplementary Fig. 2). Thus, this compound is an IFN-α-like small molecule, but the mechanism of the RO8191 antiviral activity remained unknown. Therefore, we examined the JAK/STAT activation pathway, which includes key players in the IFN signaling cascade.

Like type I IFNs, RO8191 significantly phosphorylates and activates STATs, in particular, STAT1 and STAT2 (Fig. 2c). Intriguingly, in HCV replicon cells, STAT1 expression knockdown did not affect the antiviral activity of RO8191 or IFN-α, although IFN-γ activity was inhibited (Fig. 4c). These data suggest that, in addition to inducing similar gene expression, RO8191 and IFN-α exhibit similar STAT phosphorylation profiles. Although RO8191- and IFN-α-mediated antiviral activity remained constant when STAT1 expression was reduced, this could be because IFN-α signaling in HuH-7 cells requires minimal amounts of STAT1 protein and STAT1 expression was not reduced below such a critical threshold by siRNA in our system. In contrast, the inhibitory activity of RO8191 was attenuated to the same extent as that of IFN-α when the expression of other components of ISGF3 (STAT2 and IRF-9) were reduced by siRNA (Fig. 4d and e). Incidentally, STAT1 siRNA did not attenuate RO8191 or IFN activity in EMCV-infected A549 cells (supplementary Fig.14), which supports the notion that STAT2 is an essential component of type I IFN signaling[39]. Type I IFN stimulates the formation of other STAT-containing complexes, including STAT1:STAT1, STAT3:STAT3 and STAT5:STAT5 homodimers, as well as STAT1:STAT3 and STAT2:STAT6 heterodimers[40–42]. Like IFN, RO8191 induced the phosphorylation of STAT1 and STAT2, which function as a gateway to the type I IFN signal cascade, and stimulated the phosphorylation of STAT3, 5 and 6. Another possible cause for the fact that STAT1 knockdown did not show any effect on RO8191 inhibition could be compensation by these IFN signaling-stimulated STAT complexes. This finding matches the recent report by Perry *et al.* on the STAT dependency of IFN activity against Dengue virus, that belongs to flavivirus[43]. They showed that STAT2 mediates IFN antiviral signals even in STAT1 KO cells and they discussed the possibility that other STAT family proteins would compensate for STAT1 deficiency. In summary, with regards to the activation of transcription factors and ISG expression, RO8191 and IFN-α mediate the same pathway.

IFNs activate JAK kinases via IFN receptors to induce STAT phosphorylation. RO8191 robustly phosphorylated JAK1 (Fig. 2c) in comparison with IFN-α or -β and therefore we focused on IFNAR2 (a JAK1-binding subunit of the type I IFN receptor). As with IFN-α, the activity of RO8191 was inhibited by IFNAR2 knockdown (Fig. 3b). The suggestion that IFNAR2 is an essential molecule for RO8191-induced signal transduction is supported by the fact that an IFNAR2-deficient cell line, U5A, did not respond to RO8191. Furthermore, after IFNAR2 expression had been complemented in the U5A cells, ISG induction by both RO8191 and IFN-α recovered (Fig. 3c and d). The mechanism was directly explained by SPR spectroscopy, which showed an interaction between RO8191 and the IFNAR2 ECD (Fig. 3e). RO8191 strikingly phosphorylates the IFNAR2-associated kinase JAK1, when compared to other IFN-treated cell lysates (Fig. 2c). JAK1 siRNA expression inhibited RO8191 activity (Fig. 4a), indicating that JAK1 is also an essential molecule for RO8191 activity. Interestingly, RO8191 activity remains static when IFNAR1 expression is knocked down, unlike IFN-α activity (Fig. 3a). The IFNAR1-binding-kinase Tyk2 is not required for RO8191 activity (Fig. 4b) and Tyk2 was not phosphorylated (Fig. 2c) by RO8191. Also, RO8191 induced its signal even in the Ifnar1 KO MEF and the Tyk2-deficient cell line (Supplementary Fig.

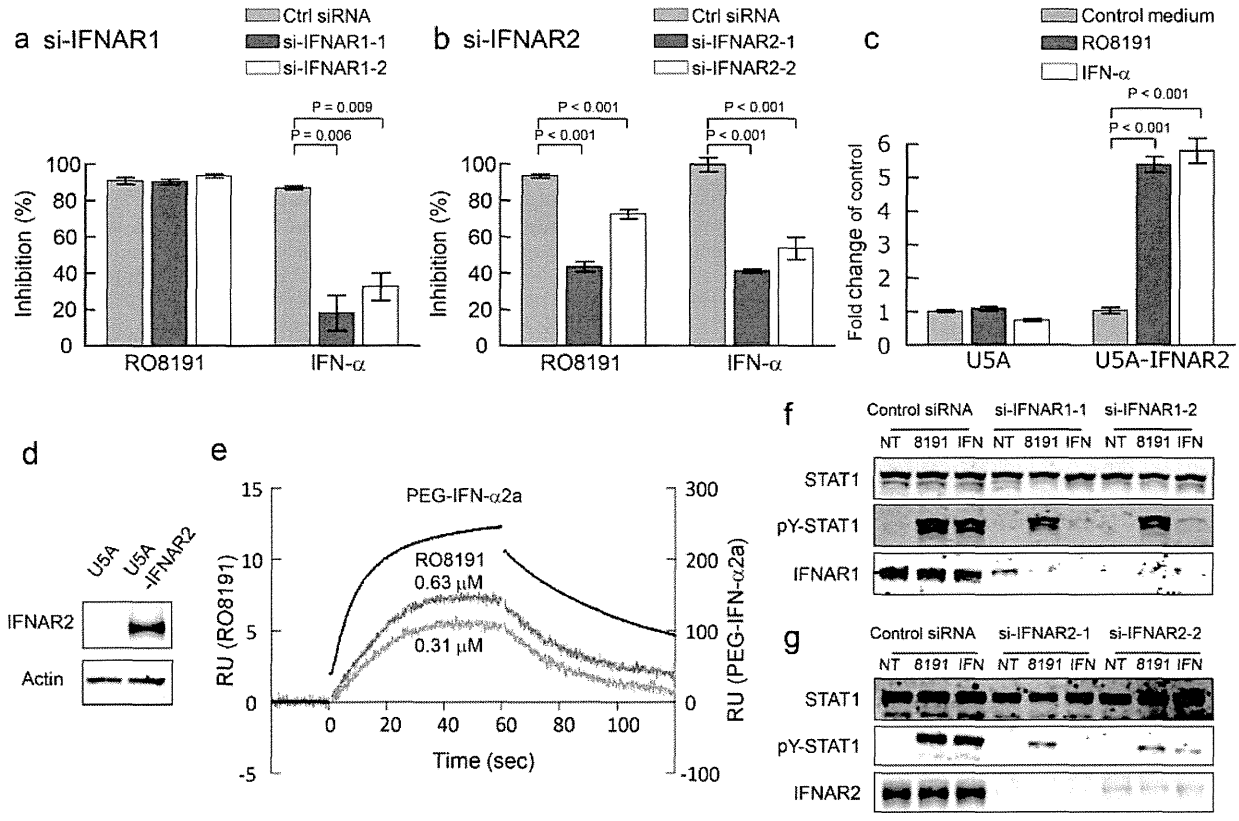


**Figure 3 | RO8191 requires and binds IFNAR2.** (a, b) The anti-HCV replicon activity of RO8191 was attenuated by knockdown of IFNAR2 (b), but not IFNAR1 (a). Inhibition of HCV replicon replication by each agent is shown (the mean and SD from 3 experiments). The HCV replicon cells were transfected with 50 nM of the indicated siRNAs (blue, red, and yellow bars). Forty-eight hours after transfection, the HCV replicon cells were treated with 1.5 μM RO8191 or 3 IU/mL IFN-α for 24 h. Twenty-four hours after treatment with each agent, the replication levels of HCV RNA were analyzed using a luciferase assay. (c, d) U5A cells that lack IFNAR2 were transfected with either an empty vector or a vector expressing the *IFNAR2* gene. (c) Forty-eight hours after transfection, the cells were treated with 50 μM RO8191 (red bars) or 100 IU/mL IFN-α (yellow bars). After an additional 8 h of incubation, total RNA was extracted from the U5A cells, and the *OAS1* mRNA level was measured using real-time RT-PCR. The values shown are relative to the mRNA level of human *β-actin*. (d) Forty-eight hours after transfection, the cells were lysed, and the whole cell lysates were immunoblotted with the indicated antibodies. (e) Real-time kinetic SPR analysis of the binding of RO8191 to the IFNAR2 ECD (red and blue lines). The results are consistent with 1:1 binding. PEG-IFN-α2a was also injected as a positive interacting control for IFNAR2 (black line, $K_D$: 30 nM). (f, g) The phosphorylation of STAT1 was attenuated by a knockdown of IFNAR2 (g) but not IFNAR1 (f). The HCV replicon cells were transfected with the indicated siRNAs (10 nM). Forty-eight hours after transfection, the cells were treated for 15 min with 10 μM RO8191 or 200 IU/mL IFN-α. The total lysates were subjected to western blot analysis to analyze the phosphorylated and total protein levels of STAT1. The data were statistically analyzed using Student's *t*-test.

8 and 11). IFN-α induces a signal via IFNAR1/Tyk2 and IFNAR2/JAK1 although RO8191 and IFN-α induce common ISGs (Fig. 2b and Supplementary Fig. 2), RO8191 activity was dependent only on IFNAR2.

We therefore propose a novel model of the induction of IFN-like signal transduction by this small molecule (Fig. 4f). So far, the IFNAR2 homodimer has been suggested to play various roles in IFN signal transduction[34,44,45], and RO8191 would induce the ISG expression via such IFNAR2 homodimer. For type I IFN, both IFNAR1 and IFNAR2 cooperate and induce phosphorylation of STATs via JAK1 and Tyk2. Conversely, for RO8191, IFNAR2 alone, as a homodimer, activates JAK1 phosphorylation and subsequent STATs activation. Experiments using siRNA and deficient cells have also shown that IFNAR1 and Tyk2 were not required to induce antiviral activity in the RO8191 compound pathway. These findings suggest a novel aspect of the IFN signaling pathway that may contribute to the understanding of other molecular signaling in IFN pathways.

RO8191 is a small molecule whose oral administration is feasible and effective in a murine model (Table 1 and Supplementary Fig. 13). In the chimeric mice study, the anti-HCV effect of RO8191 and PEG-IFN was similar in that they both showed strong activity at day 1 after treatment with subsequent weak suppression of HCV replication possibly due to the immunodeficiency of chimeric mice. Further development of RO8191 by using rational chemical modifications is therefore required to produce more potent molecules for testing as an antiviral molecule which will substitute current recombinant IFN. Although RO8191 has the potential to cause IFN-like adverse effects, further development of the small-molecule agonist offers the advantages of inexpensive production cost, convenient oral administration, dose-control to reduce some adverse effects, and potentially increased activity versus current recombinant IFNs.

Whereas oral NS3 protease inhibitors in monotherapy development yield resistant viruses[46,47], these protease inhibitors show a significantly high rate of SVR when combined with PEG-IFN[10,11] and a NS5B polymerase inhibitor also shows additive efficacy in combination with PEG-IFN[48]. In addition to the results of the *in vivo* study, we found that RO8191 induced ISGs at a level similar to IFN-α in human primary hepatocytes (Supplementary Fig. 4); we therefore expect that RO8191 will show IFN-like activity in clinical use. As an

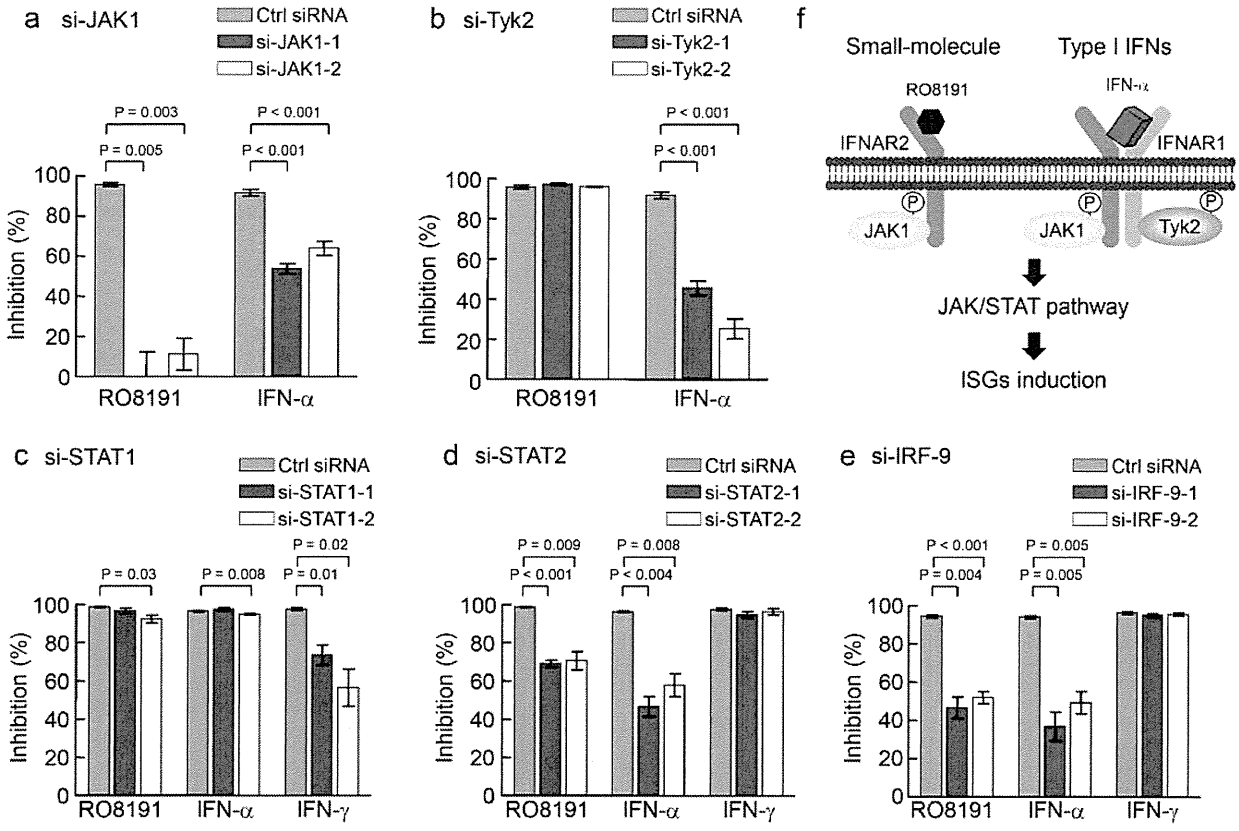


**Figure 4 | RO8191 activates a novel IFN-like pathway.** (a–e) The inhibition of HCV replicon replications by each agent is shown (mean and SD). The HCV replicon cells were transfected with 50 nM of the indicated siRNAs (blue, red, and yellow bars). (a, b) The anti-HCV replicon activity of RO8191 was reduced by knockdown of JAK1 (a) but not Tyk2 (b). Forty-eight hours after transfection, the HCV replicon cells were treated with 1.5 μM RO8191 or 3 IU/mL IFN-α. Twenty-four hours after treatment with each agent, the replication levels of HCV RNA were analyzed using a luciferase assay. (c–e) The anti-HCV replicon activity of RO8191 was reduced by knockdowns of STAT2 (d) and IRF9 (e), but not STAT1 (c). Forty-eight hours after transfection, the HCV replicon cells were treated with 1.5 μM RO8191, 3 IU/mL IFN-α, or 50 ng/mL IFN-γ. Twenty-four hours after treatment, the replication levels of HCV RNA were analyzed using a luciferase assay. (f) A schematic showing the pathways of RO8191 and IFN-α. The data were statistically analyzed using Student's *t*-test, and differences were considered significant at p values $< 0.05$.

alternative strategy to protease/polymerase inhibitors with PEG-IFN, the combined use of these direct-acting antiviral agents with RO8191 in a new oral regimen may help overcome some of the delivery problems associated with current IFNs. SVR rates of individuals infected with HCV genotype 1 have increased from 5-20% with IFN monotherapy and up to 50% with a combination of IFN and ribavirin. However, the refractory patients in this therapy constitute an unmet medical need. Thus, the development of a novel IFN receptor agonist, used alone or in combination with direct-acting antiviral drugs, will add a new milestone to the treatment of chronic hepatitis C. In addition to HCV infection, type I IFNs have been approved for the treatment of multiple clinical conditions, including hairy cell leukemia, malignant melanoma, AIDS-related Kaposi's sarcoma, multiple sclerosis, and chronic hepatitis B[49]. Thus, R08191 shows strong potential as a lead compound for IFN substitutes.

## Methods

**Cell culture, mice, and reagents.** The #Huh7/3-1 cell line, which expresses HCV replicons, was a kind gift from F. Hoffmann-La Roche. The cells were cultured in 0.5 mg/mL G418-containing Dulbecco's modified Eagle's medium (DMEM, GIBCO) supplemented with 10% fetal bovine serum (FBS, HyClone). The replicon construct was derived from pFK-I377neo/NS3-3′/WT, as previously reported[19]. Hc cells (DS Pharma Biomedical) were cultured in CSC Complete Defined Serum-Free Medium (Cell Systems Corporation) supplemented with SF4ZR-500-D Rocket Fuel. Tlr KO MEFs were purchased from OrientalBioService, Inc. Ifnar1 KO MEF was kindly gifted by Prof. Takaoka. 2fTGH, and U1A and U5A cells were kindly gifted by Prof. Stark. Culture conditions for the other cell lines are shown in Supplementary Table 5. Six-week-old C57BL/6J mice were obtained from Charles River Laboratories. Chimeric mice harboring a functional human liver cell xenograft were purchased from PhoenixBio. The protocol was reviewed by the Institutional Animal Care and Use Committee of Chugai Pharmaceutical Co., Ltd. and all mouse experiments were performed in accordance with the Guidelines for the Accommodation and Care of Laboratory Animals promulgated in Chugai Pharmaceutical Co., Ltd. Recombinant human IFN-α2a was a kind gift from F. Hoffmann-La Roche. Recombinant murine IFN-αA and human IFN-β1a were purchased from PBL Interferon Source. Recombinant TNF-α and IFN-γ were purchased from R&D Systems. Imiquimod was purchased from LKT Laboratories. JAK inhibitor I was purchased from Merck.

**Luciferase assay.** Luciferase activity was quantified using the Steady-Glo Luciferase assay system (Promega) and the EnVision 2013 Multilabel Reader (PerkinElmer).

**WST-8 assay.** The viability of drug-treated Huh-7 cells was determined using a WST-8 cell counting kit (Dojin Laboratories).

**Real-time RT-PCR.** Total RNA was extracted using Rneasy (Qiagen), and cDNA was synthesized using a Transcriptor First Strand cDNA Synthesis Kit (Roche Applied Science). Gene expression was measured using the LightCycler 480 System and LightCycler 480 Probes Master (Roche Applied Science). The amplification used 50 cycles of: 95°C for 5 min, 95°C for 10 s, and 60°C for 30 s. Human β-actin or rodent glyceraldehyde 3-phosphate dehydrogenase (GAPDH; Applied Biosystems) expression was used as the endogenous reference for each sample. Primers and TaqMan probes for genes were designed using the Universal Probe Library Assay Design Center (Roche Applied Science; Supplementary Table 6). The probes used were from the Roche Universal Probe Library (Roche Applied Science). The samples

were run in triplicate for each target gene, and each reference gene was used as an internal control.

**Western blotting and immunostaining.** Cells were lysed in CelLytic M Cell Lysis Reagent (Sigma-Aldrich) containing Protease Inhibitor Cocktail (Sigma-Aldrich) and PhosSTOP (Roche Applied Science). Rabbit polyclonal antibodies against STAT1, STAT3, STAT6, pY701-STAT1, pY690-STAT2, pY705-STAT3, pS727-STAT3, pY694-STAT5, pY641-STAT6, pY1022/1023-JAK1, and pY1054/1055-Tyk2 were purchased from Cell Signaling Technology. Rabbit polyclonal antibodies against actin, STAT2 and STAT5 were purchased from Santa Cruz Biotechnology. Anti-Tyk2 rabbit polyclonal antibody was purchased from Upstate. Anti-IFNAR1 mouse monoclonal (MAB245) and anti-IFNAR2 sheep polyclonal antibodies were purchased from R&D Systems. Anti-NS3, anti-NS5A, and anti-NS5B rabbit polyclonal antibodies were a kind gift from F. Hoffmann-La Roche. Anti-NS4A and anti-NS4B mouse monoclonal antibodies were a kind gift from the Tokyo Metropolitan Institute of Medical Science. Proteins were detected using the Odyssey Infrared Imaging System (LI-COR). For immunostaining analysis, the cells were fixed on a 35-mm glass-based dish (Iwaki) with 4% paraformaldehyde, blocked using 5% fetal bovine serum in phosphate-buffered saline, and then incubated with anti-NS3 and anti-NS4A antibodies. The cells were then washed and incubated with Alexa488-labeled anti-rabbit IgG and Alexa568-labeled anti-mouse IgG (Molecular Probes) and analyzed using confocal laser microscopy.

**JFH-1 antiviral assay.** A cured K4 cell line derived from HuH-7 HCV replicon cells was maintained in DMEM supplemented with 10% fetal calf serum (FCS), high-glucose nonessential amino acids, and HEPES (Invitrogen). The JFH-1/K4 cell line, which was persistently infected with the HCV JFH-1 strain, was maintained under the same conditions as the cured K4 cell line. For the anti-HCV assay of JFH-1/K4 cells persistently infected with the JFH-1 strain, JFH-1/K4 cells were seeded in a 24-well tissue culture plate containing DMEM supplemented with 10% FCS, high-glucose nonessential amino acids, and HEPES (Invitrogen). After overnight incubation, serial dilutions of reagent in growth medium were added. After 72 h, total RNA was purified from the JFH-1/K4 cells using Isogene (Nippon Gene). HCV-RNA was quantified by real-time PCR as previously reported[50].

**EMCV cytopathic effect assay.** This assay was performed on A549 cells seeded in a 96-well tissue culture plate containing DMEM supplemented with 10% FBS. After overnight incubation, the indicated concentrations of each reagent were added to the growth medium. After 12 h, 100 $TCID_{50}$/mL EMCV was added, and after another 48 h, viable cells were stained with 0.5% crystal violet. RNAi experiment using EMCV was also performed on A549 cells seeded in a 96-well tissue culture plate containing DMEM supplemented with 10% FBS. We transfected STAT1- or STAT2-siRNA to A549 cells, and after 72 h we infected EMCV to the cells and treated them with 1 μM RO8191 or 2 IU/mL IFN. After additional 48 h incubation, we evaluated the cell viability by staining with crystal violet.

**GeneChip and data analysis.** Total RNA was extracted from $10^7$ HCV replicon cells cultured for 8 h in the presence of 2 μM RO8191 or 4 IU/mL IFN-α with TRIzol Reagent (Invitrogen). Reverse transcription, RNA labeling (5 μg of total RNA), hybridization to Human Genome U133 Plus 2.0 Arrays (Affymetrix), and scanning were performed according to the manufacturer's instructions (Affymetrix, http://www.affymetrix.com). GC-RMA (GeneChip Robust Microarray Analysis) algorithms were used to generate scaled gene expression values. The fold change compared to untreated cells was calculated, and probe sets were selected for genes that were at least 2.0-fold upregulated in RO8191- and IFN-α-treated cells relative to the control cells.

**RNA interference.** For all double-stranded RNAs, ON-TARGET Plus siRNA reagents (Dharmacon) were used (Supplementary Table 7). The siRNAs were transiently transfected using Lipofectamine RNAiMAX Transfection reagent (Invitrogen) according to the manufacturer's protocols for reverse transfection.

**Plasmids and transfection.** ISRE and NF-κB reporter gene were purchased from Clontech. *IFNAR2* was cloned into a pCOS2 vector[51] harboring the EF1α promoter. Plasmids were transfected using FuGENE HD (Roche Applied Science) according to the manufacturer's instructions.

**SPR measurements.** SPR binding studies were performed using a Biacore T100. Recombinant IFNAR2 ECD protein was purchased from R&D Systems. The protein (1 mg/mL) was diluted 1:20 with 10 mM sodium acetate buffer (pH 5.0) and mixed with 2 μM RO8191 for stabilization of the binding site. The mixture was immobilized on a Series S sensor chip CM7 using amine coupling. RO8191 and PEG-IFN-α2a (Chugai Pharmaceutical) were injected onto the sensor chip at a flow rate of 0.03 mL/min. Response curves were generated by subtraction of the background signal generated simultaneously on a control flow cell. Kinetic parameters were obtained by global fitting of the sensorgrams to a 1:1 model using Biacore T100 Evaluation Software, version 2.0.1.

**Humanized liver mice study.** The chimeric mice were generated by transplanting human primary hepatocytes into severe combined immunodeficient (SCID) mice carrying the urokinase plasminogen activator transgene controlled by an albumin promoter[38]. The chimeric mice used in this study were applied from Inoue *et al.*[52], and had a high substitution rate of human hepatocytes. Six weeks after hepatocyte transplantation, patient serum containing $10^6$ copies of HCV genotype 1b was intravenously injected into each mouse. HCV titer reached approximately $10^8$ copies/mL and was stable after 4 weeks of HCV injection and persistently infected for 12 weeks. Here, we used mice after 5 weeks post infection and tested for 2 weeks. The mice were treated for 14 days with RO8191 30 mg/kg/day orally or PEG-IFN-α2a 30 μg/kg subcutaneously twice weekly. HCV RNA in serum was extracted using the acid guanidinium-phenol-chloroform method. Quantification of HCV RNA was performed using real-time RT-PCR based on TaqMan chemistry, as described[50]. HCV inoculations, drug administration, blood collection, and killing were performed under ether anesthesia. Blood samples were taken from the orbital vein and sera were immediately isolated. The protocols for animal experiments were approved by the local ethics committee. The animals received humane care according to NIH guidelines. Patients gave written informed consent before sampling.


1. Lavanchy, D. The global burden of hepatitis. *Liver Int.* **29**, 74–81 (2009).
2. Ghany, M. G., Strader, D. B., Thomas, D. L. & Seeff, L. B. Diagnosis, management, and treatment of hepatitis C: an update. *Hepatology.* **49**, 1335–74 (2009).
3. Zeuzem, S. Interferon-based therapy for chronic hepatitis C: current and future perspectives. *Nat Clin Pract Gastroenterol Hepatol.* **5**, 610–622 (2008).
4. Ge, D. *et al.* Genetic variation in IL28B predicts hepatitis C treatment-induced viral clearance. *Nature.* **461**, 399–401 (2009).
5. Suppiah, V. *et al.* IL28B is associated with response to chronic hepatitis C interferon-alpha and ribavirin therapy. *Nat Genet.* **41**, 1100–4 (2009).
6. Tanaka, Y. *et al.* Genome-wide association of IL28B with response to pegylated interferon-alpha and ribavirin therapy for chronic hepatitis C. *Nat Genet.***41**, 1105–9 (2009).
7. Thomas, D. L. *et al.* Genetic variation in IL28B and spontaneous clearance of hepatitis C virus. *Nature.* **461**, 798–801 (2009).
8. Czepiel, J., Czepiel, J., Biesiada, G. & Mach, T. Viral hepatitis C. *Pol Arch Med Wewn.* **118**, 734–740 (2008).
9. Webster, D. P., Klenerman, P., Collier, J. & Jeffery, K. J. Development of novel treatments for hepatitis C. *Lancet Infect Dis.* **9**, 108–117 (2009).
10. Jacobson, I. M. *et al.* Telaprevir for previously untreated chronic hepatitis C virus infection. *N Engl J Med.* **364**, 2405–16 (2011).
11. Poordad, F. *et al.* Boceprevir for untreated chronic HCV genotype 1 infection. *N Engl J Med.* **364**, 1195–206 (2011).
12. Kwong, A. D., McNair, L., Jacobson, I. & George, S. Recent progress in the development of selected hepatitis C virus NS3.4A protease and NS5B polymerase inhibitors. *Curr Opin Pharmacol.* **8**, 522–531 (2008).
13. Stark, G. R. *et al.* How cells respond to interferons. *Annu Rev Biochem.* **67**, 227–264 (1998).
14. de Veer, M. J. *et al.* Functional classification of interferon-stimulated genes identified using microarrays. *J Leukoc Biol.* **69**, 912–20 (2001).
15. Pestka, S., Langer, J. A., Zoon, K. C. & Samuel, C. E. Interferons and their actions. *Annu Rev Biochem.* **56**, 727–777 (1987).
16. Uze, G., Lutfalla, G. & Gresser, I. Genetic transfer of a functional human interferon alpha receptor into mouse cells: cloning and expression of its cDNA. *Cell.* **60**, 225–234 (1990).
17. Novick, D., Cohen, B. & Rubinstein, M. The human interferon alpha/beta receptor: characterization and molecular cloning. *Cell.* **77**, 391–400 (1994).
18. Lohmann, V. *et al.* Replication of subgenomic hepatitis C virus RNAs in a hepatoma cell line. *Science.* **285**, 110–113 (1999).
19. Sakamoto, H. *et al.* Host sphingolipid biosynthesis as a target for hepatitis C virus therapy. *Nat Chem Biol.* **1**, 333–337 (2005).
20. Wakita, T. *et al.* Production of infectious hepatitis C virus in tissue culture from a cloned viral genome. *Nat Med.* **11**, 791–796 (2005).
21. Kneteman, N. M. *et al.* Anti-HCV therapies in chimeric scid-Alb/uPA mice parallel outcomes in human clinical application. *Hepatology.* **43**, 1346–1353 (2006).
22. Dash, S. *et al.* Interferons alpha, beta, gamma each inhibit hepatitis C virus replication at the level of internal ribosome entry site-mediated translation. *Liver Int.* **25**, 580–594 (2005).
23. Der, S. D., Zhou, A., Williams, B. R. & Silverman, R. H. Identification of genes differentially regulated by interferon alpha, beta, or gamma using oligonucleotide arrays. *Proc Natl Acad Sci U S A.* **95**, 15623–15628 (1998).
24. Hemmi, H. *et al.* Small anti-viral compounds activate immune cells via the TLR7 MyD88-dependent signaling pathway. *Nat Immunol.* **3**, 196–200 (2002).
25. Kawai, T. & Akira, S. Toll-like receptor and RIG-I-like receptor signaling. *Ann N Y Acad Sci.* **1143**, 1–20 (2008).
26. Yamamoto, M. *et al.* Role of adaptor TRIF in the MyD88-independent toll-like receptor signaling pathway. *Science.* **301**, 640–3 (2003).
27. Hoshino, K. *et al.* Cutting edge: Toll-like receptor 4 (TLR4)-deficient mice are hyporesponsive to lipopolysaccharide: evidence for TLR4 as the Lps gene product. *J Immunol.* **162**, 3749–52 (1999).
28. Hemmi, H. *et al.* A Toll-like receptor recognizes bacterial DNA. *Nature.* **408**, 740–5 (2000).
29. Mosca, J. D. & Pitha, P. M. Transcriptional and posttranscriptional regulation of exogenous human beta interferon gene in simian cells defective in interferon synthesis. *Mol Cell Biol.* **6**, 2279–83 (1986).

30. Diaz, M. O. *et al.* Homozygous deletion of the alpha- and beta 1-interferon genes in human leukemia and derived cell lines. *Proc Natl Acad Sci U S A.* **85**, 5259–63 (1988).
31. Chen, H. M. *et al.* Critical role for constitutive type I interferon signaling in the prevention of cellular transformation. *Cancer Sci.* **100**, 449–56 (2009).
32. Lutfalla, G. *et al.* Mutant U5A cells are complemented by an interferon-alpha beta receptor subunit generated by alternative processing of a new member of a cytokine receptor gene cluster. *EMBO J.* **14**, 5100–5108 (1995).
33. Velazquez, L. Fellous, M. Stark, G. R. & Pellegrini, S. A protein tyrosine kinase in the interferon alpha/beta signaling pathway. *Cell.* **70**, 313–22 (1992).
34. Lewerenz, M. Mogensen, K. E. & Uzé, G. Shared receptor components but distinct complexes for alpha and beta interferons. *J Mol Biol.* **282**, 585–99 (1998).
35. Shuai, K. *et al.* Interferon activation of the transcription factor Stat91 involves dimerization through SH2-phosphotyrosyl peptide interactions. *Cell.* **76**, 821–828 (1994).
36. Sarasin-Filipowicz, M. *et al.* Interferon signaling and treatment outcome in chronic hepatitis C. *Proc Natl Acad Sci U S A.* **105**, 7034–9 (2008).
37. Farnsworth, A. *et al.* Acetaminophen modulates the transcriptional response to recombinant interferon-beta. *PloS One.* **5**, e11031 (2010).
38. Mercer, D. F. *et al.* Hepatitis C virus replication in mice with chimeric human livers. *Nat Med.* **7**, 927–33 (2001).
39. Leung, S. *et al.* Role of STAT2 in the alpha interferon signaling pathway. *Mol Cell Biol.* **15**, 1312–1317 (1995).
40. Li, X. *et al.* Formation of STAT1-STAT2 heterodimers and their role in the activation of IRF-1 gene transcription by interferon-alpha. *J Biol Chem.* **271**, 5790–4 (1996).
41. Ghislain, J. J. & Fish, E. N. Application of genomic DNA affinity chromatography identifies multiple interferon-alpha-regulated Stat2 complexes. *J Biol Chem.* **271**, 12408–13 (1996).
42. Gupta, S. Jiang, M. & Pernis, A. B. IFN-alpha activates Stat6 and leads to the formation of Stat2:Stat6 complexes in B cells. *J Immunol.* **163**, 3834–41 (1999).
43. Perry, S. T., Buck, M. D., Lada, S. M., Schindler, C. & Shresta, S. STAT2 Mediates Innate Immunity to Dengue Virus in the Absence of STAT1 via the Type I Interferon Receptor. *PloS Pathogens.* **7**, e1001297 (2011).
44. Pattyn, E. *et al.* Dimerization of the interferon type I receptor IFNaR2-2 is sufficient for induction of interferon effector genes but not for full antiviral activity. *J Biol Chem.* **274**, 34838–45 (1999).
45. Platis, D. & Foster, G. R. Activity of hybrid type I interferons in cells lacking Tyk2: a common region of IFN-alpha 8 induces a response, but IFN-alpha2/8 hybrids can behave like IFN-beta. *J Interferon Cytokine Res.* **23**, 655–66 (2003).
46. McHutchison, J. G. *et al.* Telaprevir with peginterferon and ribavirin for chronic HCV genotype 1 infection. *N Engl J Med.* **360**, 1827–38 (2009).
47. Hézode, C. *et al.* Telaprevir and peginterferon with or without ribavirin for chronic HCV infection. *N Engl J Med.* **360**, 1839–50 (2009).
48. Kneteman, N. M. *et al.* HCV796: A selective nonstructural protein 5B polymerase inhibitor with potent anti-hepatitis C virus activity in vitro, in mice with chimeric human livers, and in humans infected with hepatitis C virus. *Hepatology.* **49**, 745–52 (2009).
49. Gutterman, J. U. Cytokine therapeutics: lessons from interferon alpha. *Proc Natl Acad Sci U S A.* **91**, 1198–1205 (1994).
50. Takeuchi, T. *et al.* Real-time detection system for quantification of hepatitis C virus genome. *Gastroenterology.* **116**, 636–642 (1999).
51. Yabuta, N. *et al.* Method for screening ligand having biological activity. PCT Int. Appl. WO0206838 (2002).
52. Inoue, K. *et al.* Evaluation of a cyclophilin inhibitor in hepatitis C virus-infected chimeric mice in vivo. *Hepatology.* **45**, 921–8 (2007).

## Acknowledgments

This study was supported financially by Chugai Pharmaceutical Co., Ltd. H.K., K.O., Y.O., H.Y., H.O., M.A., A.O., H.S., N.H., A.K., K.M., T.T., N.S., Y.A., M.A. and M.S. are employees of Chugai Pharmaceutical Co., Ltd. We are grateful to George Stark for providing us the 2fTGH, U1A and U5A cell lines, and Akinori Takaoka for mouse Ifnar1-knockout MEFs. We also thank Isamu Kusanagi and Chiaki Tanaka for technical assistance, AVSS Co., Ltd. for technical assistance on EMCV, and Editing Services at Chugai Pharmaceutical Co., Ltd. for editorial assistance.

## Author contribution statement

H.K., K.O., Y.O., H.Y., Y.H., A.O. and N.H. performed the experiments; H.K., K.O., H.O. and M.A. analyzed the data; G.F. and W.A. provided experimental materials and input into the data analysis; H.S., A.K., M.K., T.T., N.S., G.F., Y.A., M.A. and M.S. provided expert information; and H.K. and M.S. wrote the manuscript.

## Additional information

**Supplementary information** accompanies this paper at http://www.nature.com/scientificreports

**Competing financial interests:** The authors declare no competing financial interests.



**How to cite this article:** Konishi, H. *et al.* An orally available, small-molecule interferon inhibits viral replication. *Sci. Rep.* **2**, 259; DOI:10.1038/srep00259 (2012).

Arch Virol (2011) 156:295–304
DOI 10.1007/s00705-010-0859-x

ORIGINAL ARTICLE

# Establishment of infectious HCV virion-producing cells with newly designed full-genome replicon RNA

**Masaaki Arai · Hidenori Suzuki · Yoshimi Tobita · Asako Takagi · Koichi Okamoto · Atsunori Ohta · Masayuki Sudoh · Michinori Kohara**

Received: 27 January 2010 / Accepted: 30 October 2010 / Published online: 19 January 2011


**Abstract** Hepatitis C virus (HCV) replicon systems enable in-depth analysis of the life cycle of HCV. However, the previously reported full-genome replicon system is unable to produce authentic virions. On the basis of these results, we constructed newly designed full-genomic replicon RNA, which is composed of the intact 5′-terminal-half RNA extending to the NS2 region flanked by an extra selection marker gene. Huh-7 cells harboring this full-genomic RNA proliferated well under G418 selection and secreted virion-like particles into the supernatant. These particles, which were round and 50 nm in diameter when analyzed by electron microscopy, had a buoyant density of 1.08 g/mL that shifted to 1.19 g/mL after NP-40 treatment; these figures match the putative densities of intact virions and nucleocapsids without envelope. The particles also showed infectivity in a colony-forming assay. This system may offer another option for investigating the life cycle of HCV.

M. Arai · A. Takagi
Pharmacology Research Laboratories I,
Mitsubishi Tanabe Pharma Corporation,
1000, Kamoshida-cho, Aoba-ku, Yokohama 227-0033, Japan

M. Arai · Y. Tobita · M. Kohara (✉)
Infectious Diseases Project, The Tokyo Metropolitan Institute of Medical Science, 1-6, Kamikitazawa, 2-chome, Setagaya-ku, Tokyo 156-8506, Japan
e-mail: kohara-mc@igakuken.or.jp

H. Suzuki
Laboratory for Electron Microscopy, Tokyo Metropolitan Institute of Medical Science, 1-6, Kamikitazawa, 2-chome, Setagaya-ku, Tokyo 156-8506, Japan

K. Okamoto · A. Ohta · M. Sudoh
Kamakura Research Laboratories, Chugai Pharmaceutical Co., Ltd., 200 Kajiwara, Kamakura, Kanagawa 247-8530, Japan

## Introduction

Hepatitis C virus (HCV) is a major cause of chronic hepatitis, liver cirrhosis, and hepatocellular carcinoma. With over 170 million people currently infected [2], HCV is a growing public-health burden.

The life cycle of HCV has been difficult to study because cell culture and small animal models of HCV infection are not available. The recent development of HCV replicon systems has permitted the study of HCV translation and RNA replication in human hepatoma-derived Huh-7 cells in vitro [17]. However, these replicon systems cannot produce authentic virions because they lack the infection steps, and analysis of these infection steps is very important for understanding HCV pathogenesis.

Recently, some groups have successfully established in vitro infection systems [16, 21, 26, 28–30]. The strategies of these systems are basically the same as the ones used for transfection of Huh-7 cells or their derivatives with in vitro-generated HCV genome RNA [1]. The non-structural regions used in those studies were from the 2a genotype JFH (Japan Fulminant Hepatitis)-1 clone or the 1a genotype H77 clone. The former is known for its exceptionally vigorous amplification and broad permissiveness in cultured cells other than Huh-7 [3, 12, 13], while the latter shows only poor replication ability. Another group reported a newly established immortalized hepatocyte cell line that is susceptible to HCV infection, but only modest improvement was achieved [10]. There are also reports of a system using a full-genome replicon that has the entire coding region under the control of the internal ribosomal entry site of encephalomyocarditis virus, EMCV-IRES; however, this system also failed to show infectivity in the G418 selection assay [7, 20], and secretion of particles with the putative characteristics of HCV virions could not be confirmed [4].

We now report the establishment of infectious virion-producing replicon cells that utilize an ordinary genotype 1b replicon strain. In order to address the contribution of structural and non-structural gene products to the maturation of HCV particles in vitro, we partitioned these regions in the same cistron of the full genomic sequence, thereby enabling the functions of these structural and non-structural genes to be studied separately. Thus, we termed this construction "divided open reading frame carrying" full genome replicon, or dORF replicon.

Virus particles secreted from cells containing dORF replicon RNA, as confirmed morphologically using electron microscopy, were shown to be able to infect Huh-7 cells. Replication of dORF replicon RNA was so efficient that infected cells could survive and proliferate under G418 selection to form colonies, as seen after transfection with replicon RNA. In addition, a reporter gene was successfully inserted into the construct, and activity of the reporter gene could be transmitted to naive Huh-7 cells by infection.

We believe that the success of this system is due to the difference in the construction of the replicon, namely, having the intact 5′ half extending to NS2 instead of being divided at the beginning of the core region. Although further investigation is required to elucidate whether the encapsidation signal of HCV is located in the region that is divided in the full-genome replicon, this is the first report to describe genome-length replicon-containing cells that can produce virus particles that have the putative characteristics of the HCV virion, in terms of both morphology and biological properties.

## Results

### dORF replicon RNA can replicate in Huh-7 cells

We began this study with transfection with the dORF replicon RNAs (Fig. 1A). When 30 μg of each RNA was electroporated into $4 \times 10^6$ Huh-7 cells, the dORF and dORF bla RNA-transfected cells formed 20 and 5 colonies, respectively, after 3 weeks of G418 selection. No colonies appeared as a result of transfection with polymerase-defective mutants (data not shown). Two colonies were picked, amplified, and designated as dORF replicon cell #1 and #2, and dORF bla replicon cell #1 and #2. Some of these cells were then used for quantification of HCV RNA and northern blot analysis (Fig. 1B). Northern blot analysis showed that these clones contained HCV RNAs of the expected size and that the HCV RNA copy numbers of these clones did not differ substantially from that of the subgenomic replicon, indicating that replication ability had not been hampered by insertion of the structural genes, which is counter to what was expected. Western blot analysis showed that these clones express both structural and non-structural proteins (Fig. 1C). These results confirmed that transfected dORF HCV RNAs can replicate in Huh-7 cells, just as authentic subgenomic replicon RNAs do.

### dORF replicon cells secrete virus particles

In a previous study, HCV subgenomic replicon cells secreted RNase-resistant subgenomic RNA into the culture supernatant [4, 7, 20]. We also detected a similar amount of RNase-resistant HCV RNA in the culture supernatant of our dORF replicon cells, as well as of the subgenomic and full-genome replicon cells. These supernatants showed no significant differences in terms of distribution of HCV RNA in buoyant density gradient analysis (Figs. 2A, B, open square). In contrast, there was a clear difference between these supernatants after NP-40 treatment. While almost all of the HCV RNA in the supernatant of the subgenomic replicon cells was eliminated by NP-40 treatment (Fig. 2A, filled triangle), there remained a peak of HCV RNA at a density of 1.18 g/mL in the supernatant of the dORF replicon cells (Fig. 2B, filled triangle). These results were confirmed in the same experiment, using concentrated culture supernatant (Figs. 2C, D). We also confirmed the results of previous reports [7, 20], which showed no genomic RNA resistant to NP-40 treatment in the supernatant of full-genome replicon cells (Fig. 2E). Secreted core proteins in the concentrated supernatant showed a different density gradient distribution compared to genomic RNA (Fig. 2F, open circle) in that the core proteins were present at densities of 1.1–1.2 g/mL, while HCV RNA was more broadly distributed in the range of 1.06–1.22 g/mL. Thus, HCV RNA and core proteins were not always associated with each other. However, after NP-40 treatment, core proteins were found only in the same fraction as HCV RNA, at 1.19 g/mL (Fig. 2F, filled triangle). Taken together with the results of the report mentioned above [20], our replicon cells harboring dORF RNA appeared to secrete particles with core proteins that were assembled into nucleocapsids as well as particles without core proteins that were sensitive to NP-40 treatment, like the ones from subgenomic and full-genome replicon cells. We concluded that the broader distribution of the HCV genome RNA in the density gradient than that of the core protein was caused by the overlapping distribution of these two particle types, and that the remaining peaks of genome RNA and core protein after NP-40 treatment were of nucleocapsids that had had their envelopes stripped off by NP-40 [11].

According to our hypothesis, the distribution of core proteins in the density gradient represented that of the

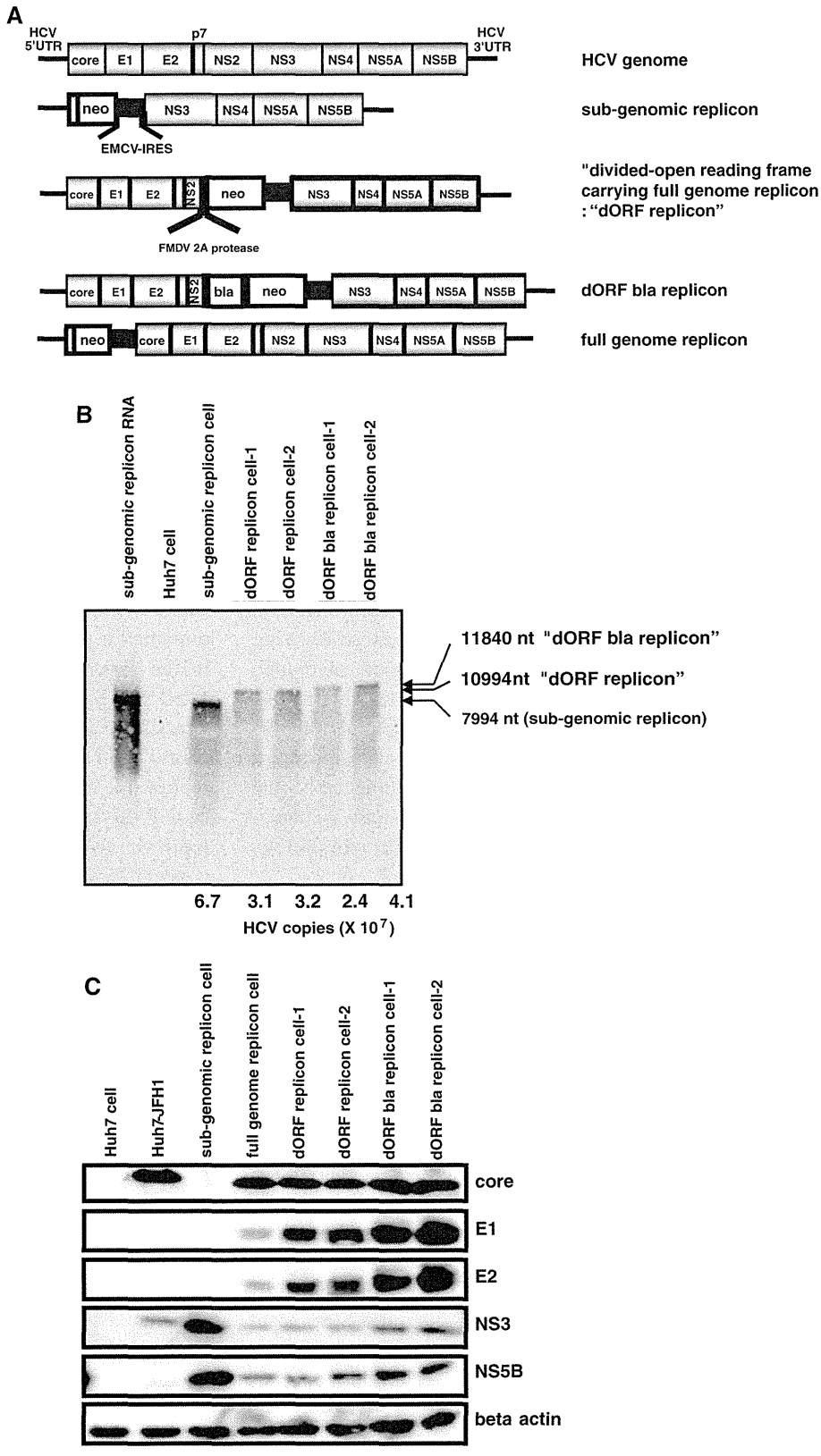


**Fig. 1** Confirmation of "divided open reading frame carrying" (dORF) replicon cells. (A) Schematic representations of replicon RNAs used in this study. All the replicon constructs contained inserts just after the T7 promotor. UTR, untranslated region; NS, non-structural protein; neo, neomycin phosphotransferase II; EMCV, encephalomyocarditis virus; IRES, internal ribosomal entry site; FMDV, foot-and-mouth disease virus; bla, beta-lactamase. (B) Northern blot analysis. A 10-μg amount of total RNA from each cell sample was loaded. Subgenomic replicon RNA: $10^8$ copies of in vitro-generated subgenomic RNA. Numbers below the lanes are the HCV copy number per microgram of total RNA. Huh-7 cell, subgenomic replicon cell, dORF replicon cell #1, #2, dORF bla replicon cell #1, #2. (C) Western blot analysis. A 10-μg amount of each cell lysate was loaded. Huh-7 cell, Huh-7-JFH1: Huh-7 cell transfected with JFH1 viral RNA, subgenomic replicon cell, full-genome replicon cell, dORF replicon cell #1, #2, dORF bla replicon cell #1, #2

intact virion, and we therefore tried to observe virions directly by electron microscopy, using the fraction in which the core protein was present. We easily identified numerous round-shaped virus particles approximately 50 nm in diameter by scanning electron microscopy (Fig. 3A). Furthermore, when the immunogold method using anti-E2

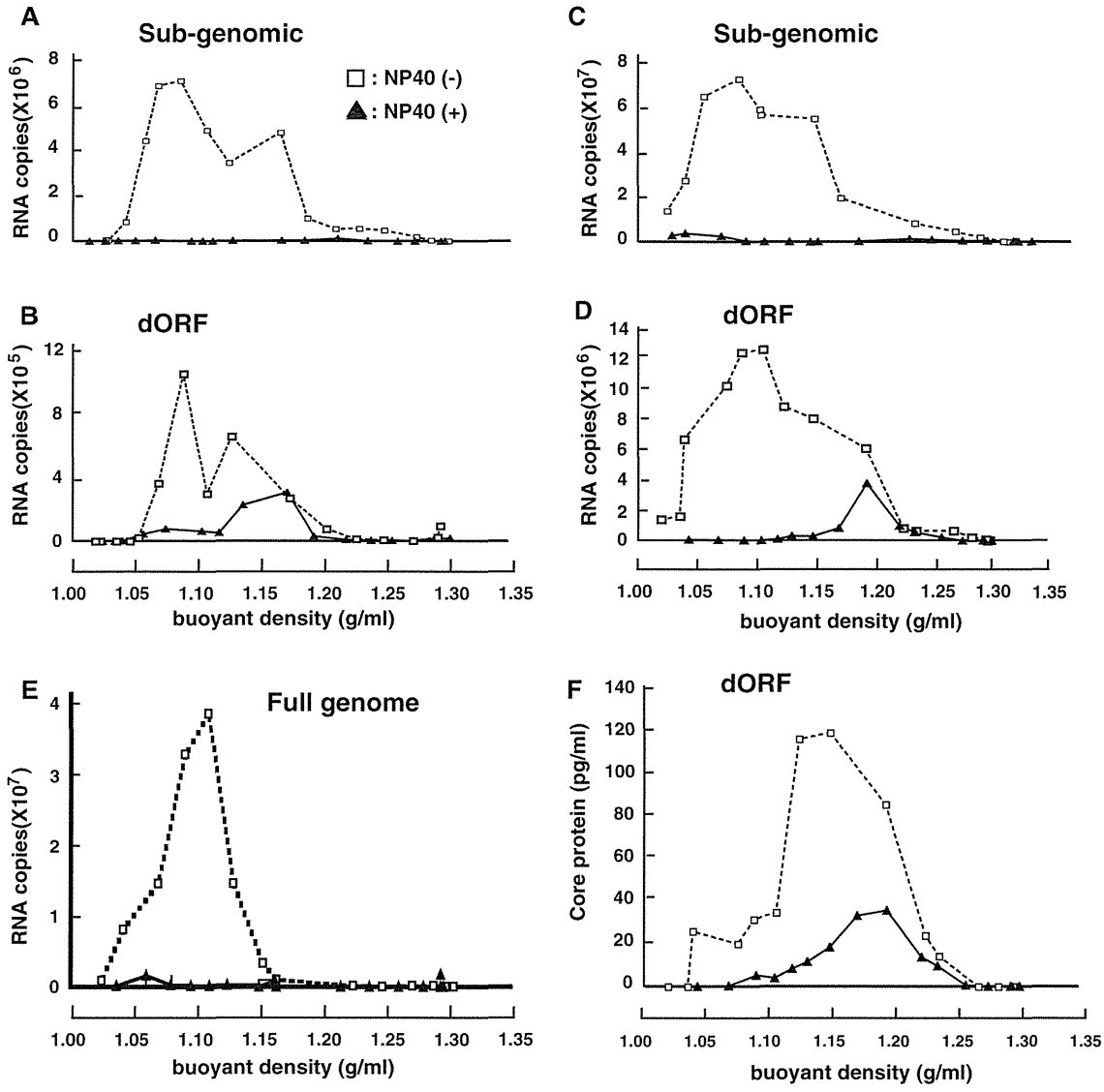


**Fig. 2** Density gradient analysis of supernatants. Culture supernatants were treated with RNaseA and loaded directly onto a sucrose density gradient without treatment (open square) or after NP-40 treatment (filled triangle). Quantification of HCV RNA in each fraction of supernatant from the subgenomic replicon (A) and dORF replicon (B). Analysis of concentrated culture supernatant from the subgenomic replicon (C) and dORF replicon (D). Concentrated culture supernatant from the full-genome replicon NNC#2 was also analyzed (E). Quantification of HCV core protein in each fraction of supernatant from the dORF replicon (F)

RR6 antibody was applied to samples fixed on the mesh, transmission electron microscopy could be used to visualize virus particles labeled with colloidal gold (Fig. 3B). These findings provide evidence of intact virion production from our dORF replicon cells.

Secreted virus particles can infect naive Huh-7 cells

Next, we examined the infectivity of these virus particles. The culture supernatants of these dORF replicon cells were collected, and 3 kinds of naive Huh-7 cells, one purchased from the J.C.R.B. (Japanese Collection of Research Bioresources) and the other two, designated as the cured cells F2 and K4, generated by IFN-α treatment of 1bneo/delS replicon cells, were infected with these supernatants. After two sequential passages and three weeks of G418 selection as described above, a number of colonies appeared, as shown in Fig. 4A. The largest number of colonies was produced from the cured cells K4, and slightly fewer colonies were produced from the cured cells F2, while no colonies appeared when normal Huh-7 cells were used (data not shown). The same infection experiment carried

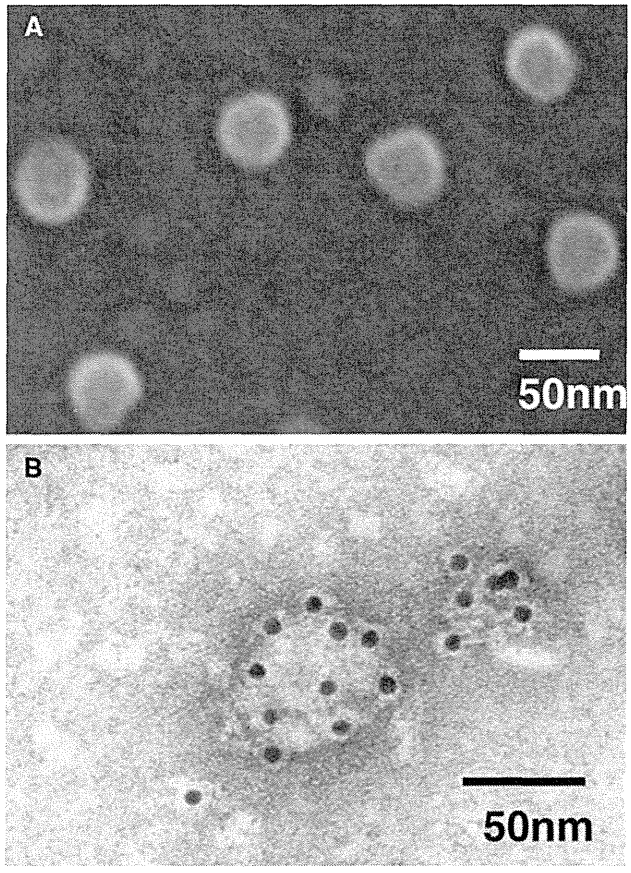


**Fig. 3** Electron microscopy analysis of virus-like particles. The core-protein-rich fraction collected from the density gradient was further concentrated by ultracentrifugation and observed by scanning electron microscopy (A). The same fraction attached to formvar-coated grids was incubated with rabbit anti-E2 RR6 antibody, treated with goat anti-rabbit IgG coupled to 10-nm colloidal gold, negatively stained with uranyl acetate, and then examined by transmission electron microscopy (B)

out with full-genome replicon cells produced no infectivity in the supernatant (data not shown). Under the most efficient conditions, the titer of the supernatant reached as high as 20 cfu (colony-forming units) per milliliter when the putative doubling time of these cells was approximately 24 h. Furthermore, the appearance of colonies was abolished by addition of the antibody JS-81 (BD Pharmingen), an antibody to CD81, a possible co-receptor of HCV [22] (Fig. 4B).

Next, we propagated some of these colonies for further analysis. Northern blot analysis showed that these clones carry HCV RNAs of reasonable size (Fig. 5A), including subgenomic RNA (7994 bases), dORF RNA (10994 bases), and dORF bla RNA (11840 bases). Western blot analysis revealed that the cell clones that were infected with supernatant from Huh-7 cells containing the dORF replicon expressed structural proteins (Fig. 5B), indicating that the colonies were not just the reappearance of subgenomic replicons hidden in the cured cells.

Together, our findings indicate that these particles in the supernatant infected the Huh-7 cells through a CD81-associated pathway and that infected cells formed colonies after G418 selection, similar to what was observed with electroporation with subgenomic RNA.

### A reporter gene inserted into the dORF replicon RNA can be transmitted through infection

First, we confirmed that the beta-lactamase gene in the dORF bla replicon RNA was active in established replicon cell clones and able to process the green fluorescent substrate into blue fluorescent product (Fig. 6A). Next, we attempted to detect the activity of the beta-lactamase gene in the cloned infected colonies. Three clones grown from cells infected with the dORF bla supernatant were treated using a GeneBLAzer In Vivo Detection Kit. One clone was positive for blue fluorescence (Fig. 6B), demonstrating that a reporter gene inserted into the dORF replicon could be transmitted to naive Huh-7 cells through secreted virus particles in the culture supernatant.

## Discussion

There have been several previous reports of full-genome HCV replicons that can replicate well in Huh-7 cells and express sufficient amounts of structural proteins [1, 4, 7, 14, 20]. Pietschmann et al. (2002) observed the secretion of an RNase-resistant HCV genome into the supernatant from both full-genome and subgenomic replicon cells and non-specific uptake of these genomes by naive Huh-7 cells. Ikeda et al. (2002) were also unable to detect any infectivity in the supernatant of their full-genome replicon cells. They assumed that the reason for this failure was the inability of Huh-7 cells to release intact virions or to be infected by the virus, although this was later demonstrated not to be the case by a series of reports on infection using the JFH-1 clone [16, 26, 30].

First, we attempted to improve the efficiency of the full-genome replicon in two ways, namely, by modifying the construct and reducing the genome size. Numerous studies have examined the encapsidation signal in the genomic RNA of positive-sense single-stranded viruses [5, 8, 9]. Frolova et al. [5] showed that the encapsidation signal of Sindbis virus lies in the nsP1 gene and is 132 nucleotides long. Johansen et al. [9] found that the IRES of poliovirus had the ability to enhance the efficiency of packaging of the polio subgenomic replicon. We think that these findings indicate that the construction of the genome could affect the efficacy of encapsidation, and we therefore decided to

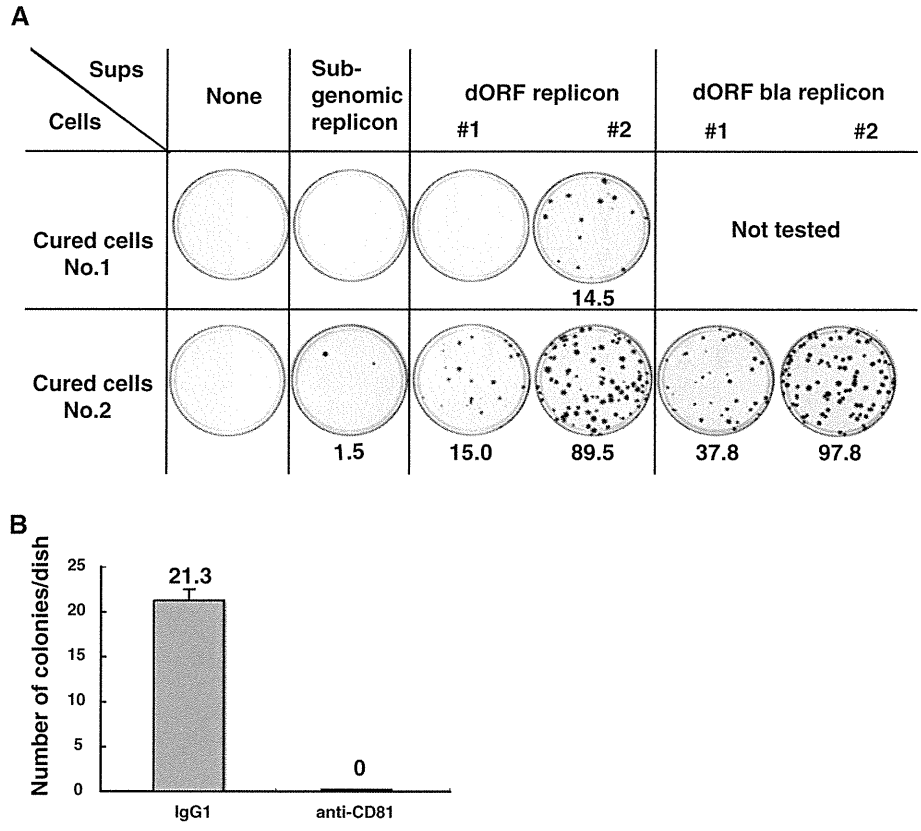


**Fig. 4** Infectivity of supernatants from various replicon cells. Colonies of cells infected with the indicated supernatant. Numbers shown below the plates are the average of a total of four plates per condition (A). Inhibition of infection by anti-CD81 antibody. Cured cell K4 cells (No.2 in Fig. 4A) were treated with mouse IgG1 as the negative control or anti-CD81 before infection (B)

change the site of genome division from the beginning of the core region to the middle of the NS2 region. Regarding the size of the genome, there have been reports that the insertion of a foreign gene of significant size can result in the deletion of a portion of the chimeric genome during replication [18, 19]. We therefore removed the second half of the NS2 region, because this region appears to be unnecessary for both replication and packaging in Huh-7 cells, and this deletion was found to have no influence on the efficacy of encapsidation, as there were no apparent differences between the NS2-deleted construct and the one containing the entire NS2 region (data not shown).

Our established dORF replicon was able to replicate well in Huh-7 cells and express sufficient amounts of structural proteins, similar to the previously reported full-genome replicon. Although both the dORF replicon cells and the previously reported full-genome replicons secreted RNase-resistant genomes, there was a striking difference between these two full-genome replicons when NP-40 treatment was carried out on their supernatants. There was no RNase-resistant genome left in the NP-40-treated supernatant of full-genome replicons, although density gradient analysis of the NP-40-treated supernatant of dORF replicon cells clearly showed the coexistence of the HCV genome and core proteins at a peak of 1.18 g/mL. This peak may represent NP-40-resistant nucleocapsids. The distribution of core proteins in the density gradient analysis of the concentrated supernatant of the dORF replicons did not match that of the HCV genome. A reasonable explanation for this mismatch is that the lighter side of the broad peak of the HCV genome was not representative of intact virions and is instead an indication of secretion by a pathway used in subgenomic replicon cells, which differs from the natural process. The fact that the peak of the HCV genome of full-genome replicons was located in a narrow range on the lighter side compared to that of the dORF replicons supports this hypothesis. We observed round particles in the concentrated core protein fraction using electron microscopy, and those particles also seemed to contain core proteins. These findings indicate that our dORF replicon cells produced both intact virions and artificial membranous particles, with the former having the morphological and biophysical characteristics of putative virions.

The colony-forming assay clearly demonstrated the ability of the supernatants of our dORF replicon cells to infect Huh-7 cells efficiently. The reason for the difference in efficacy between the two cured cells is uncertain but may involve the ability to support replication or the level of receptor expression. This needs to be clarified in order to improve the efficiency of HCV infection in vitro. Differences in the efficiency of infection were also noted between

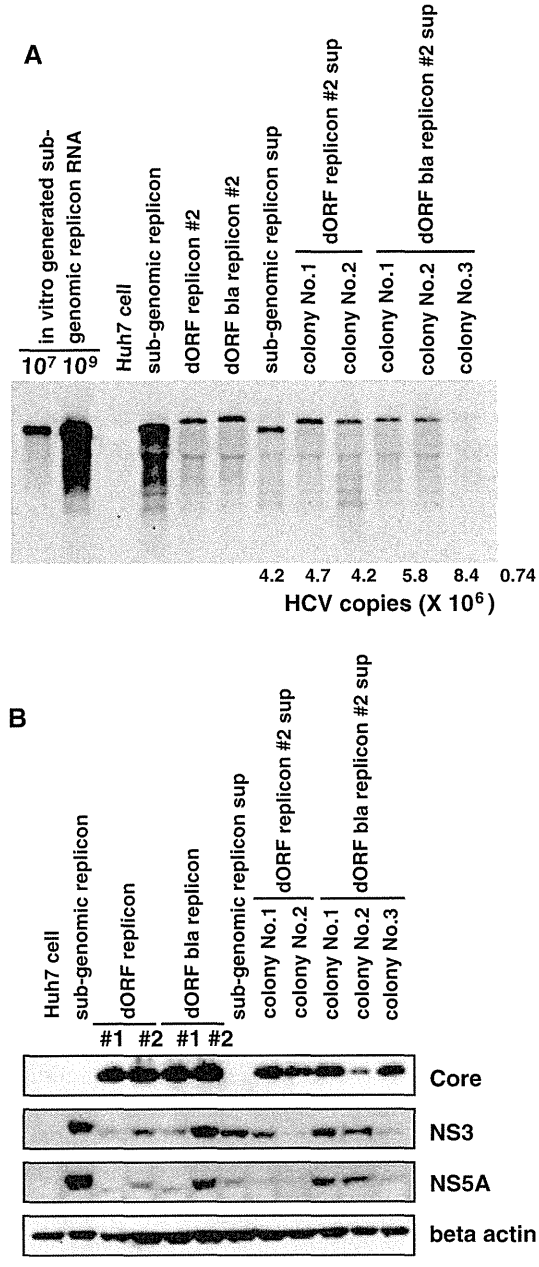


**Fig. 5** Northern blot analysis of colonies formed after infection. $10^7$, $10^9$: amounts of in vitro-generated subgenomic replicon RNA loaded. Numbers below the lanes are the HCV copy number per μg of total RNA (A). Huh-7 cells, subgenomic replicon cells, dORF replicon cell #2, dORF bla replicon cell #2, subgenomic replicon sup: colony from cells transduced with subgenomic replicon supernatant, colony No.1, 2 of dORF replicon #2 sup: colonies from cells infected with dORF replicon #2 supernatant, colony No.1, 2, and 3 of dORF bla replicon #2 sup: colonies from cells infected with dORF bla replicon #2 supernatant. Western blot analysis of colonies formed after infection (B). The order of the lanes is identical to that for the northern blot, except for the dORF and dORF bla replicons, which represent two clones in this figure

clones of the same dORF replicon cells, which may have been due to the accumulation of different mutations in the structural region, although we have not yet confirmed this

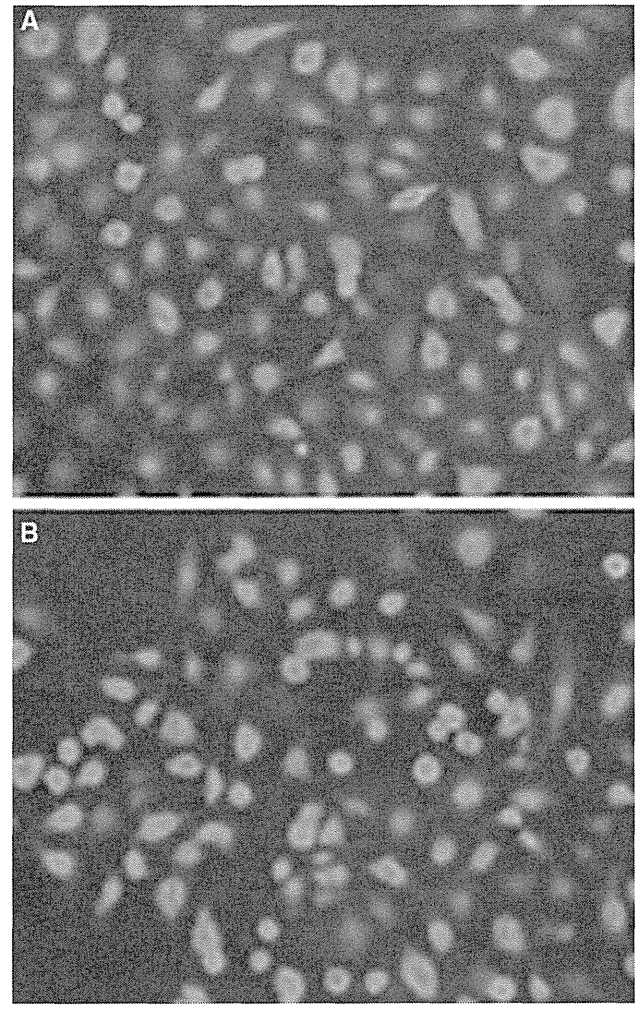


**Fig. 6** Detection of beta-lactamase activity in dORF replicon cells. Parental dORF bla replicon #2 cell (A) and colony no. 3 cloned from cells infected with dORF bla replicon #2 cell supernatant (B). Blue fluorescence shows high beta-lactamase activity, indicating that the reporter gene functioned normally after infection

hypothesis. We also observed colonies being formed by cells that were treated with supernatant containing subgenomic replicons, and these colonies most likely represent the so-called "non-specific transduction" of the subgenomic replicon. Although this dORF supernatant infection could be blocked by the anti-CD81 antibody reported previously [30], we cannot exclude the possibility that the infection we observed was due to highly efficient "non-specific transduction," as we could not determine whether "non-specific transduction" also could be affected by the anti-CD81 antibody because of the low colony-forming ability of the supernatant of subgenomic replicons.

We also demonstrated that the reporter gene that was inserted in addition to the neomycin resistance gene could be transmitted to the new generation of viruses. This finding raises the possibility of producing sufficient amounts of reporter virus constitutively.

In summary, we established an infectious-particle-producing HCV replicon system. This achievement should yield more precise information about the encapsidation signal of HCV, which was kept intact despite the partitioning of the genome. This system also allows analysis of the pathway of HCV infection, including adsorption of virions to cell-surface receptors, penetration, uncoating, virus particle assembly, and HCV release. Moreover, the dORF replicon system may be used as a convenient tool to investigate the utility of the newly established siRNA system [14, 27] and evaluation of compounds that are effective against subgenomic replicons.

Although we believe that the reason for our success is our new construct, further examination is necessary to verify our findings.

## Materials and methods

### Construction and RNA transcription

To construct dORF replicon RNA, the second half of the NS2 region of the HCV-R6 strain [25] was replaced in frame with the foot and mouth disease virus (FMDV) 2A protease gene, the neomycin resistance gene, and the encephalomyocarditis virus (EMCV) internal ribosomal entry site (IRES). In addition, the region from NS3 to the beginning of NS5B was replaced with the 1bneo/delS replicon sequence from the N strain of genotype 1b [6](kindly provided by Dr. Seeger). This construct was designated as the "divided open reading frame carrying full genome" (dORF) replicon. The subgenomic replicon construct was also prepared from the R6 strain and also contained the 1bneo/delS replacement. For the reporter assay, the FMDV 2A protease gene and beta-lactamase gene (bla; Invitrogen) were inserted after the remaining NS2 gene to produce the dORF bla replicon construct. Replication-deficient versions of these three replicons were also prepared by deleting 27 nucleotides, including the GDD motif of NS5B polymerase.

In vitro transcription of these replicon RNAs was performed using the MEGAscript kit (Ambion).

### Cell culture and electroporation

Huh-7 cells were cultured in DMEM (SIGMA) with 10% fetal bovine serum. Replicon cells were maintained in the same medium supplemented with 300 μg/mL G418 (Invitrogen). These cells were passaged 3 times a week at a 4:1 splitting ratio. Electroporation of replicon RNA was performed as described previously [17]. The subgenomic replicon (1bneo/delS replicon) cells were treated with 1000 IU of IFN-α for 2 months and cloned by the limited dilution method. Two of these clones were designated as HCV replicon-cured Huh-7 cells F2 and K4. The cell line containing the full-genome replicon of genotype1b, namely the NNC#2 clone [15], was a kind gift from Dr. Shimotohno of Keio University.

### Northern blot analysis and quantification of HCV RNA

Total RNA was purified from cells using ISOGEN (Nippon Gene) for northern blot analysis or ABI prizm6100 (Applied Biosystems) for real-time RT-PCR. Purified RNAs were quantified by absorbance at 260 nm. For northern blot analysis, 30 μg of each total RNA was used with a Northern Max Kit (Ambion) according to the manufacturer's instructions. The probe for detection of HCV RNA was a PCR fragment of the NS5B region (nucleotide numbers 7629–7963) that had been biotin-labeled using a BrightStar Psoralen-Biotin Kit (Ambion) according to the manufacturer's instructions. Following hybridization of the membranes, the probe was detected using a BrightStar BioDetect Kit (Ambion) according to the manufacturer's instructions, and luminescence was detected using the LAS1000 detection system (Fujifilm). Measurement of the HCV RNA copy number by real-time RT-PCR was performed using an ABI PRISM 7900 system (Applied Biosystems) as described previously [24].

### Western blot analysis

Western blot analysis was carried out using the conventional semi-dry blot method. Cells were lysed with buffer containing 100 mM Tris-HCl (pH 7.4) and 4% sodium dodecyl sulfate. A 10-μg amount of protein from each sample was separated by SDS-PAGE through a 4–20% gradient gel (Invitrogen) and transferred to the membrane according to the gel manufacturer's protocol. The antibodies used in this study were anti-core mouse monoclonal antibody (MAb), anti-E1 MAb, anti-E2 MAb (reported previously; [25]), anti-NS3 antiserum (reported previously; [25]), anti-NS5B antiserum (Upstate), and anti-beta-actin MAb (Abcam). Horseradish peroxidase-labeled anti-mouse and anti-rabbit IgG goat antibodies (Santa Cruz Biotechnology and DAKO, respectively) were used as the secondary antibody. The membranes were treated using an ECL Plus kit (Amersham) according to the manufacturer's instructions, and luminescence was detected using an LAS1000 system (Fujifilm).

### Density gradient analysis and core ELISA

Culture supernatants from replicon cells were loaded onto 10–60% sucrose density gradient tubes with or without 10-fold concentration in an Amicon-100 (Millipore). The

tubes were then ultracentrifuged at 100,000 *g* for 16 h and fractionated. NP-40 was added to the culture supernatants to a final concentration of 0.5%, and they were then incubated at 4°C for 30 min. For electron microscopy, the culture supernatant was concentrated, loaded onto a 60% sucrose cushion, and ultracentrifuged at 100,000 *g* for 4 h. The interface between the concentrated medium and the sucrose cushion was collected and separated by the density gradient method described above. A 2-mL fraction from 5 ml to 7 mL from the bottom, with a density of 1.1–1.2 g/mL, was examined by electron microscopy after further concentration by the sucrose cushion ultracentrifugation method described above. The amount of core protein in the fractions was quantified using an Ohso ELISA kit in accordance with the manufacturer's instructions.

### Electron microscopy

The concentrated fraction of core protein was observed by scanning and transmission electron microscopy. For scanning electron microscopy, the sample was allowed to settle on the surface of a poly-L-lysine-coated glass cover slip for 30 min, and the attached sample was then fixed with 0.1% glutaraldehyde in 0.1 M phosphate buffer (pH 7.4) for 10 min, washed three times with 0.1 M phosphate buffer, and post-fixed with 1% osmium tetroxide in the same buffer for 10 min. After dehydration through a graded series of ethanol, the samples were dried in a freeze dryer (Hitachi ES-2020, Hitachi) using t-butyl alcohol, coated with osmium tetroxide, approximately 2 nm thick, using an osmium plasma coater (NL-OPC80; Nippon Laser and Electronics Laboratory), and then examined using a Hitachi S-4800 field emission scanning electron microscope at an accelerating voltage of 10 kV [23]. For transmission electron microscopy, the sample was allowed to settle on a formvar-coated nickel grid for 10 min, dried in air, incubated with rabbit anti-E2RR6 antibody (prepared as described in the supplementary information), washed with PBS, and then incubated with goat anti-rabbit IgG coupled to 10-nm colloidal gold (British BioCell). After negative staining with 2% uranyl acetate, the sample was examined using a JEM 1200EX transmission electron microscope (JEOL) at an accelerating voltage of 80 kV.

Rabbit anti-E2 RR6 antibody to the HCV-E2 protein was prepared as follows: The E2 gene of HCV type 1b [25] was cloned under the control of the ATI-P7.5 hybrid promoter of vaccinia virus vector pSFB4 and allowed to recombine with the Lister strain of the vaccinia virus to give vector RVV. Rabbits were infected intradermally with $10^8$ p.f.u. of RVV, and 2 months later, they received two booster injections with the purified E2 protein. HCV-E2 protein was expressed from the RVV vector and purified by lentil lectin column chromatography and affinity chromatography using an anti-E2 monoclonal antibody [25].

### Infection

A 2.5-ml aliquot of cleared culture supernatants from replicon cells was added to approximately 70% confluent of Huh-7 cells in 25-$cm^2$ flasks, and the same amount of complete DMEM was added 2 h later. Infected cells were transferred to 75-$cm^2$ flasks the next day and to four 10-cm dishes 2 days later. G418 at a concentration of 300 μg/mL was added to the medium immediately after the second passage. The three types of Huh-7 cells used in this study included the one purchased from J.C.R.B. and the 2 IFN-cured replicon cell lines F2 and K4 described above. The medium was changed every other day. For the blocking experiment, cells were treated with the anti-CD81antibody as described previously [30]. Cells were fixed with 10% formalin/PBS(-) for 10 min after washing with PBS(-) and staining with 1% crystal violet/PBS(-) for 1 h before washing with water.

### Beta-lactamase detection assay

Beta-lactamase activity was detected using a GeneBLAzer In Vivo Detection Kit (Invitrogen) according to the manufacturer's instructions and observed using a fluorescence microscope (Nikon) with UV light excitation.

**Acknowledgments** The authors would like to thank Dr. Christoph Seeger of the Fox Chase Cancer Center for providing the 1bneo/delS replicon plasmid and Dr. Kunitada Shimotohno of Keio University for providing full-genome genotype 1b replicon clone NNC#2. We also thank Etsuko Endo for her secretarial work and Dr. Masahiro Shuda for fruitful discussions. This study was supported in part by grants from the Ministry of Education, Culture, Sports, Science and Technology of Japan, the Program for Promotion of Fundamental Studies in Health Sciences of the National Institute of Biomedical Innovation of Japan, and the Ministry of Health, Labour and Welfare of Japan.



## References

1. Blight KJ, McKeating JA and Rice CM (2002) Highly permissive cell lines for subgenomic and genomic hepatitis C virus RNA replication. J Virol 76:13001-13014
2. Choo QL, Kuo G, Weiner AJ, Overby LR, Bradley DW and Houghton M (1989) Isolation of a cDNA clone derived from a blood-borne non-A, non-B viral hepatitis genome. Science 244:359-362
3. Date T, Kato T, Miyamoto M, Zhao Z, Yasui K, Mizokami M and Wakita T (2004) Genotype 2a hepatitis C virus subgenomic

replicon can replicate in HepG2 and IMY-N9 cells. J Biol Chem 279:22371-6
4. Date T, Miyamoto M, Kato T, Morikawa K, Murayama A, Akazawa D, Tanabe J, Sone S, Mizokami M and Wakita T (2007) An infectious and selectable full-genome replicon system with hepatitis C virus JFH-1 strain. Hepatol Res 37:433-443
5. Frolova E, Frolov I and Schlesinger S (1997) Packaging signals in alphaviruses. J Virol 71:248-258
6. Guo J, Bichko VV and Seeger C (2001) Effect of alpha interferon on the hepatitis C virus replicon. J Virol 75:8516-8523
7. Ikeda M, Yi M, Li K and Lemon SM (2002) Selectable subgenomic and genome-length dicistronic RNAs derived from an infectious molecular clone of the HCV-N strain of hepatitis C virus replicate efficiently in cultured Huh7 cells. J Virol 76:2997-3006
8. Jia X-Y, Van Eden M, Busch MG, Ehrenfeld E and Summers DF (1998) Trans-encapsidation of a poliovirus replicon by different picornavirus capsid proteins. J Virol 72:7972-7977
9. Johansen LK and Morrow CD (2000) The RNA encompassing the internal ribosome entry site in the poliovirus 5′ nontranslated region enhances the encapsidation of genomic RNA. Virology 273:391-399
10. Kanda T, Basu A, Steele R, Wakita T, Ryerse JS, Ray R and Ray RB (2006) Generation of infectious hepatitis C virus in immortalized human hepatocytes. J Virol 80:4633-4639
11. Kanto T, Hayashi N, Takehara T, Hagiwara H, Mita E, Naito M, Kasahara, A, Fusamoto H and Kamada T (1994) Buoyant density of hepatitis C virus recovered from infected hosts: two different features in sucrose equilibrium density-gradient centrifugation related to degree of liver inflammation. Hepatology 19:296-302
12. Kato T, Furusaka A, Miyamoto M, Date T, Yasui K, Hiramoto J, Nagayama K, Tanaka T and Wakita T (2001) Sequence analysis of hepatitis C virus isolated from a fulminant hepatitis patient. J Med Virol 64:334-339
13. Kato T, Date T, Miyamoto M, Furusaka A, Tokushige K, Mizokami M and Wakita, T (2003) Efficient replication of the genotype 2a hepatitis C virus subgenomic replicon. Gastroenterology 125:1808-1817.
14. Kim M, Shin D, Kim SI and Park M (2006) Inhibition of hepatitis C virus gene expression by small interfering RNAs using a tricistronic full-length viral replicon and a transient mouse model. Virus Res 122:1-10
15. Kishine H, Sugiyama K, Hijikata M, Kato N, Takahashi H, Noshi T, Nio Y, Hosaka M, Miyanari Y, Shimotohno K (2002) Subgenomic replicon derived from a cell line infected with the hepatitis C virus. Biochem Biophys Res Commun 293:993-9
16. Lindenbach BD, Evans MJ, Syder AJ, Wolk B, Tellinghuisen TL, Liu C C, Maruyama T, Hynes RO, Burton DR, McKeating JA and Rice CM (2005) Complete replication of hepatitis C virus in cell culture. Science 309:623-626
17. Lohmann V, Korner F, Koch J, Herian U, Theilmann L and Bartenschlager R (1999) Replication of subgenomic hepatitis C virus RNAs in a hepatoma cell line. Science 285:110-113
18. Lu, HH, Alexander L and Winner E (1995) Construction and genetic analysis if dicistronic Polioviruses containing open reading frames for epitopes of Human Immunodeficiency Virus type 1 gp120. J Virol 69:4797-4806
19. Mattion NM, Reilly PA, DiMichele SJ, Crowley JC and Weeks-Levy C (1994) Attenuated poliovirus strain as a live vector: expression of regions of rotavirus outer capsid protein VP7 by using recombinant Sabin 3 viruses. J Virol 68:3925-3933
20. Pietschmann T, Lohmann V, Kaul A, Krieger N, Rinck G, Rutter G, Strand D and Bartenschlager R (2002) Persistent and transient replication of full-length hepatitis C virus genomes in cell culture. J Virol 76:4008-4021
21. Pietschmann T, Kaul A, Koutsoudakis G, Shavinskaya A, Kallis S, Steinmann E, Abid K, Negro F, Dreux M, Cosset FL and Bartenschlager R (2006) Construction and characterization of infectious intragenotypic and intergenotypic hepatitis C virus chimeras. Proc Natl Acad Sci USA 103:7408-7413
22. Pileri P, Uematsu Y, Campagnoli S, Galli G, Falugi F, Petracca R, Weiner AJ, Houghton M, Rosa D, Grandi G and Abrignani S (1998) Binding of hepatitis C virus to CD81. Science 282:938-941
23. Suzuki H, Murasaki K, Kodama K and Takayama H (2003) Intracellular localization of glycoprotein VI in human platelets and its surface expression upon activation. Bri J Haematol 121:904-912
24. Takeuchi T, Katsume A, Tanaka T, Abe A, Inoue K, Tsukiyama-Kohara K, Kawaguchi R, Tanaka S and Kohara M (1999) Real-time detection system for quantification of hepatitis C virus genome. Gastroenterology 116:636-42
25. Tsukiyama-Kohara K, Tone S, Maruyama I, Inoue K, Katsume A, Nuriya H, Ohmori H, Ohkawa J, Taira K, Hoshikawa Y, Shibasaki F, Reth M, Minatogawa Y and Kohara M (2004) Activation of the CKI-CDK-Rb-E2F pathway in full genome hepatitis C virus-expressing cells. J Biol Chem 279:14531-14541
26. Wakita T, Pietschmann T, Kato T, Date T, Miyamoto M, Zhao Z, Murthy K, Habermann A, Krausslich HG, Mizokami M, Bartenschlager R and Liang TJ (2005) Production of infectious hepatitis C virus in tissue culture from a cloned viral genome. Nat Med 11:791-796
27. Watanabe T, Sudoh M, Miyagishi M, Akashi H, Arai M, Inoue K, Taira K, Yoshiba M and Kohara M (2006) Intracellular-diced dsRNA has enhanced efficacy for silencing HCV RNA and overcomes variation in the viral genotype. Gene Ther 13:883-92
28. Yi MK and Lemon SM (2004) Adaptive mutations producing efficient replication of genotype 1a Hepatitis C virus RNA in normal Huh7 cells. J Virol 78:7904-7915
29. Yi MK, Villanueva RA, Thomas D, Wakita T and Lemon SM (2006) Production of infectious genotype 1a hepatitis C virus (Hutchinson strain) in cultured human hepatoma cells. Proc Natl Acad Sci USA 103:2310-2315
30. Zhong J, Gastaminza P, Cheng G, Kapadia S, Kato T, Burton DR, Wieland SF, Uprichard SL, Wakita T and Chisari FV (2005) Robust hepatitis C virus infection in vitro. Proc Natl Acad Sci USA 102:9294-9299